Food & Function

ROYAL SOCIETY OF CHEMISTRY

PAPER

View Article Online
View Journal | View Issue

Cite this: *Food Funct.*, 2021, **12**, 1156

Inulin ameliorates schizophrenia *via* modulation of the gut microbiota and anti-inflammation in mice†

Li Guo, ‡[a] Peilun Xiao,‡[b] Xiaoxia Zhang,[c] Yang Yang, [a] Miao Yang,[a] Ting Wang,[a] Haixia Lu,[d] Hongyan Tian,[a] Hao Wang *[a] and Juan Liu *[a]

The microbiome–gut–brain (MGB) axis, which regulates neurological and cognitive functions, plays an essential role in schizophrenia (SCZ) progression. Dietary inulin could be a novel strategy for the treatment of SCZ due to its modulating effects on the gut microbiota. In this study, the effects of inulin on mice with SCZ were studied. As indicated by the behavioural tests, expression of neurotransmitters, inflammatory indicators, and brain morphology, inulin administration ameliorated aberrant behaviours (locomotor hypoactivity, anxiety disorders and depressive behaviours, and impaired learning and spatial recognition memory) and effectively reduced neuroinflammation and neuronal damage. In addition, inulin improved intestinal integrity and permeability, as indicated by the elevated expression of tight junction proteins ($p < 0.05$). The results of 16S rRNA sequencing and analysis showed that inulin increased the abundance of *Lactobacillus* and *Bifidobacterium*, which were negatively correlated with 5-hydroxytryptamine and inflammatory cytokines and positively correlated with brain-derived neurotrophic factor (BDNF). Inulin caused a reduction in *Akkermansia* that was positively correlated with inflammatory cytokines and negatively correlated with BDNF. These results suggested that dietary inulin modulated the gut microbiota and exerted anti-inflammatory effects in mice though the MGB axis, which further ameliorated SCZ. Therefore, the results of this study provide a potential explanation for inulin intervention in the treatment of SCZ.

Received 23rd October 2020,
Accepted 15th December 2020

DOI: 10.1039/d0fo02778b

rsc.li/food-function

1. Introduction

Schizophrenia (SCZ) is a heterogeneous neurodevelopmental disorder that is characterised by psychosis. With a worldwide incidence of approximately 1%,[1] it has become one of the global leading causes of disability and imposes significant socioeconomic burdens on public health.[2] Unfortunately, effective psychopharmacological options remain limited.[3] The aetiology of schizophrenia is complicated and assumed as multifactorial, including genetic dysfunction, prenatal and/or postnatal environmental risk factors, *etc.*[4–8] Due to its complexity, the underlying mechanism of SCZ pathogenesis is yet to be completely understood. Increasing research has implicated the potential role of the 'microbiome-gut-brain (MGB) axis' in SCZ attributed to the gut microbiome regulating the bidirectional signalling between the central nervous system (CNS) and enteric nervous system.[9] Accumulating evidence has indicated that the MGB axis signalling influences neurotransmission, neurogenesis, myelination, dendrite formation and blood–brain barrier development, as well as modulates cognitive function and behavioural patterns.[10–12] Perturbation of microbiota and microbial metabolites can modulate the behaviour in mouse.[13,14] Conversely, neurological and neurodevelopmental disorders could result in changes in the gut microbiota.[15] Considering the role of the gut microbiota in the gut inflammatory response, it is highly conceivable that the gut microbiota contribute to the pathogenesis of SCZ by influencing the immune system and the inflammatory response. Recently, the effects of neuroinflammation[16] and microbiota dysfunction[17,18] have been observed in the pathogenesis of SCZ. Therefore, the importance of neuroinflammation and the involvement of microbiota in SCZ have received great attention. This might inspire researchers to develop novel strategies for the treatment of SCZ.

[a]*School of Basic Medical Sciences, Ningxia Medical University, Yinchuan 750004, Ningxia, China. E-mail: 568587854@qq.com, yyibr@hotmail.com, 623755794@qq.com, wangting950417@126.com, 664593460@qq.com, wanghaograduate@126.com, ryuken0518@163.com; Tel: +86 15825311426, +86 13995073111*

[b]*Department of Anatomy, Weifang Medical University, Weifang 261042, Shandong, China. E-mail: xiaopeilun123@sina.com*

[c]*College of Traditional Chinese Medicine, Ningxia Medical University, Yinchuan 750004, Ningxia, China. E-mail: zxx1216@163.com*

[d]*Clinical Medical College, Ningxia Medical University, Yinchuan 750004, Ningxia, China. E-mail: 739899841@qq.com*

†Electronic supplementary information (ESI) available. See DOI: 10.1039/d0fo02778b

‡These authors contributed equally to this work.

Inulin, a natural fructan, has been widely used in food, pharmaceuticals, and many other fields as dietary fiber and a prebiotic.[19] A variety of biological functions of inulin have been demonstrated, including regulating immune and metabolism and balancing intestinal microbiota, thus contributing to a partial reversal or remission of several diseases. For instance, it can alleviate type 2 diabetes mellitus (T2DM)[20,21] and lipid metabolism disorders[22] by suppressing inflammation and modulating the gut microbiota. Furthermore, inulin prevents inflammatory bowel disease (IBD) by modulating the colonic production of short-chain fatty acids (SCFAs) and suppressing mucosal inflammation.[23] Inulin also influenced the activity of intestinal microbiota in the prevention of colon cancer development.[24] In our previous studies, we have shown that inulin ameliorated alcoholic liver disease (ALD) by suppressing the lipopolysaccharide (LPS)-toll-like receptor-4 (TLR-4)-Mψ axis[25] and modulating the gut microbiota *via* SCFA-induced suppression of M1 and facilitation of M2 macrophages in mice.[26] The beneficial effect of inulin was reported to be its selective stimulation of some bacteria, such as *Lactobacillus*, *Bifidobacterium*,[23] and *Prevotellaceae.*[22] However, the effect of inulin on the MGB axis has yet to be elucidated.

In addition to functioning as a prebiotic in indirectly modulating the intestinal immune response, inulin is recognized by intestinal epithelial cells and it directly stimulates the release of anti-inflammatory cytokines. Therefore, a significant prospective application of inulin could be predicted for the treatment of diseases related to both intestinal microbial imbalance and immune dysfunction. Thus, considering the simultaneous occurrence of inflammation and microbial imbalance in SCZ, inulin could be a desirable candidate for its treatment. However, the exact effects and mechanisms of dietary inulin on SCZ remain largely unknown.

This study investigated whether inulin can ameliorate SCZ by modulating the gut microbiota and suppressing the microglial activation *via* the MGB axis in a murine model, which may contribute to the theoretical foundation of inulin intervention in the treatment of CNS diseases.

2. Materials and methods

2.1 Animals and diets

Six-week old male C57BL/6J mice, obtained from Vital River Laboratory Animal Technology Co., Ltd (Beijing, China, license number: SCXK [Beijing] 2016-0011), were caged at room temperature (22 ± 1 °C) and air humidity of 40–60%, with a 12 h light/dark cycle. Modified drinking water with inulin or risperidone was provided to the mice. Inulin (product number: Q/P&H0001S; purity: 91%) was purchased from Fengning Ping'an High-tech Industrial Co., Ltd, Chengde, China, and risperidone (product number: H 20065005) was purchased from Siyao Pharmaceuticals Co., Ltd, Changzhou, China. All animal experimental procedures were approved by the Ethics Committee of Ningxia Medical University (no. 2014-014).

2.2 Experimental design

Sixty male C57BL/6J mice (6 weeks old, weighing 19 ± 1 g) were randomly allocated to the following four groups (15 mice per group): (a) model mice group with schizophrenia (SCZ): intraperitoneally injected with MK-801 0.6 mg per kg body weight daily for 14 consecutive days and fed a normal diet;[27] (b) SCZ with inulin group (INU + SCZ): after MK-801 administration, mice were fed drinking water containing inulin (2 g per kg body weight) for 6 weeks as the intervention group;[28] (c) SCZ with risperidone group (RIP + SCZ): after MK-801 administration, mice were fed drinking water containing risperidone (0.1 mg per kg body weight) for 6 weeks as the positive control group;[29] and (d) control group (CON): mice were intraperitoneally injected with an equal volume of saline for 14 days and fed a normal diet. Drinking water was freshly prepared with inulin powder or risperidone solution daily. The average daily volume of liquid intake per mouse was monitored. After 8 weeks (14 days of modelling and 6 weeks of drinking water intervention), their faeces were collected. Prior to euthanisation, the mice were subjected to behavioural tests, and the associated indications were investigated.

2.3 Behavioural tests

2.3.1 Open-field test (OFT). Mice were placed individually at the centre of the unfamiliar arena (40 cm × 40 cm × 40 cm) and allowed to explore it freely for 6 min. Their spontaneous activities over the last 5 min were recorded using an automatic video tracking system (Smart version 3.0; Panlab, S.L.U., Barcelona, Spain). The arena was divided into two areas: the central zone (25% of the inner surface area, far away from the walls) and the peripheral zone (75% of the outer surface area, outside the centre). The total travelled distance was considered as an index of locomotor activity. Rearing and defecation were considered as indices of 'anxiety levels', while increased proportion of distance or time spent in the central zone indicated decreased anxiety. In order to eliminate the odour left by the previous mice, their urine was cleaned with 75% alcohol before each mouse was subjected to the open field test.

2.3.2 Morris water maze (MWM) assay. Morris water maze (MWM) testing was conducted in a round pool (90 cm in diameter and 40 cm in depth). The pool was filled to a depth of 11 cm with water-based white non-toxic titanium dioxide paint. The pool and room temperatures were maintained at 24 ± 1 °C. The escape platform was a 25 cm^2 plexiglass square, placed at the centre of one quadrant of the pool, 15 cm from the pool's edge, and submerged 1 cm beneath the water surface. The platform remained in the same position throughout the learning trials in navigation training, and it was removed from the pool during the spatial probe test.

At the beginning, each mouse was placed gently into the pool facing the wall at one of the four positions (north, south, east, and west), and four quadrant tests were completed daily for the first 4 days. The maximum swim time was set at 60 s. If the mouse located the platform within 60 s and stayed on it for up to 10 s, it was immediately removed from the pool. If not, the mouse was gently guided to the platform to reorient to

the cues for an additional 30 s before being removed from the pool. Mice were then dried to keep them warm. On day 5, the navigation training began and the escape incubation period of mice within 60 s in each quadrant was recorded. To examine their spatial reference memory, a spatial probe test was performed 24 h after the navigation training. During the spatial probe test, the platform was removed from the pool and the mouse was lowered into the water from the opposite quadrant of the original platform position, allowed to swim freely for 60 s, and the number of times it crossed the platform was recorded. The SMART digital tracking system (version 2.5, Panlab, Barcelona, Spain) was simultaneously used to record the trial.

2.4 Blood samples and tissue preparation

Blood samples were collected in tubes containing ethylenediaminetetraacetic acid and centrifuged (at 1500*g* for 10 min) to obtain plasma samples. All plasma samples were stored at −80 °C for further analysis. The plasma C-reactive protein (CRP) and LPS levels were determined using an automatic biochemical analyser (HITACHI, 7180, Tokyo, Japan) and a limulus amebocyte lysate kit (Bioendo Technology Co., Ltd, Xiamen, China), respectively.

The whole brain and a part of the small intestine tissues were isolated. One half of the samples were used for enzyme-linked immunosorbent assay (ELISA) determination of neurotransmitters and inflammatory cytokines, while the other half were fixed with 4% paraformaldehyde for immunohistochemistry, Nissl staining, and hematoxylin and eosin (HE) staining.

2.5 Enzyme-linked immunosorbent assay (ELISA)

The concentrations of 5-hydroxytryptamine (5-HT), dopamine (DA) (Elabscience Biotechnology, China), brain-derived neurotrophic factor (BDNF), tumour necrosis factor-α (TNF-α), interleukin (IL)-1β, IL-6, and IL-10 (Cloud-Clone Corp., China) were detected by ELISA. A commercial kit was used to measure each cytokine level in plasma or the supernatants of brain tissues according to the manufacturer's instructions. Briefly, the brain tissues were rinsed with ice-cold phosphate-buffered saline (PBS; 0.01 M, pH = 7.4) to remove any excess blood. They were then weighed, minced, and homogenized in PBS with an automatic sample freeze-grinding instrument (JXFSTPRP-CL, Shanghai Jingxin Industrial Development Co., Ltd, China) at 0 °C. The homogenates were then centrifuged for 5 min at 5000*g* to obtain the supernatant. The absorbance was read at 450 nm using a spectrophotometer (Varioskan LUX, Thermo Fisher Scientific, USA), and the brain sample concentrations were subsequently calculated using the equation generated from a standard curve.

2.6 Plasma lipopolysaccharide (LPS) assay

A limulus amebocyte lysate kit (Bioendo Technology Co., Ltd, Xiamen, China) was used to detect the concentration of LPS in plasma according to the manufacturer's instructions. The optical density at 545 nm was measured using a microplate reader (Thermo Fisher Scientific, Waltham, MA, USA).

2.7 Hematoxylin and eosin (HE) staining

The brain and small intestine tissues of the sacrificed mice were immediately fixed in 4% paraformaldehyde, dehydrated, and embedded in paraffin. The sections cut from the paraffin-embedded blocks were stained with HE. The slides were observed under an Olympus microscope (Aomori Olympus, BX51, Japan) to evaluate the enteric integrity, including inflammation and changes in the thickness of the intestinal mucosa, and assess inflammatory cell infiltration in the cerebral cortex. The mean length of the villi in the small intestine was measured to determine the thickness of the intestinal mucosa.

2.8 Immunohistochemistry

To determine the role of microglia and the integrity of the intestinal mucosal barrier in SCZ after inulin treatment, immunohistochemistry was used to analyze the brain and intestinal tissues. The slides were dewaxed and rehydrated. Subsequently, the slides were incubated in sodium citrate solution for 10 min and placed in a microwave oven over medium heat to unmask the antigen. The slides were dropped in 3% hydrogen peroxide for 20 min to block endogenous peroxidase and then blocked with ready-to-use goat serum for 30 min at 22 ± 2 °C. The brain slides were incubated with a rabbit anti-mouse Iba-1 antibody (1 : 8000 dilution, Abcam, no. 178847, USA), and the intestine slides were incubated with a rabbit anti-mouse occludin antibody (1 : 200 dilution, Abcam, no. 216327, USA) or a rabbit anti-mouse Zonula occludens 1 (ZO-1) antibody (1 : 100 dilution, Abcam, no. 214228, USA) at 37 °C for 1 h. After rinsing, the slides were incubated with horseradish peroxidase conjugated goat anti-rabbit immunoglobulin-G (1 : 1000 dilution, Abbkine, no. A21020, China) for 20 min at room temperature. After 3 min of reaction with substrate-chromogen 3, 3′-diaminobenzidine, the slides were counterstained with hematoxylin to observe the nucleus. Images were captured with an Olympus BX51 microscope. The positive areas in the 40× optical fields of the cerebral cortex, the hippocampal CA1, CA3, and DG regions, and the intestinal lumen mucosal region were then observed using the ImageJ software (National Institutes of Health, Bethesda, MD, USA). The observers were blinded to the experimental groups.

2.9 Nissl staining

The prepared sections were obtained from each group, dewaxed to hydration according to the previously described procedure, and then placed in a dyeing tank filled with cresyl violet stain (Nissl staining kit, Solarbio Technology, Beijing) at 56 °C for 1 h. The sections were then removed and rinsed with deionised water. Nissl differentiation solution was added to each section in turn, and the differentiation time was controlled under the microscope to achieve a complete or almost colourless background. After differentiation, the sections were rinsed with distilled water for 10 min, dehydrated with a gradient of ethanol, made transparent with xylene, and finally sealed with neutral gum. The morphological changes of

neurons in various hippocampal regions (CA1, CA3, and DG) were observed with a microscope (Bar = 20 μm).

2.10 Isolation of brain microglial cells

Microglial cells, the major inflammatory innate immune cells in the CNS, were digested and isolated from the mouse brain tissues as previously described.[30] Briefly, a whole brain tissue was minced prior to being subjected to 15 min digestion at 37 °C. The digestion mixtures used were 10 mL of 0.25% (weight by volume) type IV collagenase (Sigma, San Francisco, USA) and 20 μL DNase I (28 U mL^{-1} Sigma, D5025, San Francisco, CA, USA). Subsequently, the specimens were mashed through a 200-mesh nylon membrane (Sigma-Aldrich, S3895, Oakville, ON, Canada). The homogenate was centrifuged for 7 min at 421*g*, and then the supernatant was carefully poured off. To remove myelin, the brain homogenates were subjected to centrifugation in the presence of 10 mL of 37% (volume by volume) Percoll solution (Solarbio Technology Co., Ltd, Beijing, China) for 10 min at 500*g*. The myelin layer was sucked off and the cell pellet was retained. Then, the cells were washed by adding 1× Hank's balanced salt solution and centrifuged for 10 min at 550*g*. The cell pellets were re-suspended, washed with Dulbecco's modified Eagle's medium (DMEM), and centrifuged for 10 min at 421*g*. Finally, the samples were re-suspended in 100 μL of DMEM, and the concentration was adjusted to 1×10^7 cells per mL for flow cytometry staining.

2.11 Flow cytometry analysis

Flow cytometry staining was performed in the dark at 4 °C. The cells were re-suspended and incubated with 1 μL of CD16/CD32 (BD Biosciences, no. 214228, USA) for 15 min to block non-specific binding of antigen. Subsequently, 100 μL of suspended cells were stained with phycoerythrin (PE)-conjugated anti-mouse CD45 antibody and allophycocyanin (APC)-conjugated anti-mouse CD11b antibody (BD Biosciences, no. 553081, no. 553312, USA) for 30 min. Meanwhile, the cells were stained with isotype-matched control antibodies, respectively. Finally, the prepared samples were detected using a Cyto FLEX flow cytometer (Beckman Coulter, USA).

2.12 Gut microbiota analysis

The faecal microbial 16S ribosomal RNA (rRNA) gene sequencing and analysis were performed as described in previous studies.[14,25] After 6 weeks of drinking intervention, five mice were randomly selected from each group and transferred to separate sterilised cages to collect fresh faeces, which were immediately frozen in liquid nitrogen individually and then stored at −80 °C until DNA extraction.

Microbial genomic DNA extraction was performed using the E.Z.N.A.® Soil DNA Kit (Omega Biotek Norcross, GA, USA) according to the manufacturer's instructions. DNA extraction was checked by electrophoresis on a 1% agarose gel, and the DNA concentration and purity were determined with a NanoDrop 2000 UV-vis spectrophotometer (Thermo Scientific, Wilmington, USA). The V3 and V4 regions of the 16S rRNA gene were amplified by polymerase chain reaction (PCR) with primer pairs 338F (5′-ACTCCTACGGGAGGCAGCAG-3′) and 806R (5′-GGACTACHVGGGTWTCTAAT-3′) using an ABI GeneAmp® 9700 PCR thermocycler (ABI, CA, USA). The PCR amplification of the 16S rRNA gene was performed as follows: initial denaturation at 95 °C for 3 min, followed by 27 cycles of denaturation at 95 °C for 30 s; annealing at 55 °C for 30 s and extension at 72 °C for 45 s; and a single extension at 72 °C for 10 min and finally at 4 °C. The PCR mixtures contained 4 μL of 5× TransStart FastPfu buffer, 2 μL of 2.5 mM 2′-deoxynucleoside 5′-triphosphate, 0.8 μL of forward primer (5 μM), 0.8 μL of reverse primer (5 μM), 0.4 μL of TransStart FastPfu DNA Polymerase, 10 ng template DNA, and finally double-distilled H_2O of up to 20 μL. PCR reactions were performed in triplicate. The PCR product was extracted from 2% agarose gel using an AxyPrep DNA gel extraction kit (Axygen Biosciences, Union City, CA, USA) according to the manufacturer's instructions and then quantified using a Quantus Fluorometer (Promega, USA). In order to carry out Qubit quantification and library detection, the library was constructed using the TruSeq®DNA PCR-free sample preparation kit. After passing the test, the library was sequenced using the Illumina MiSeq (Illumina, San Diego, CA) on the cloud platform of Shanghai Majorbio Bio-pharm Technology Co., Ltd, China.

2.13 Statistical analysis

GraphPad Prism version 8 (GraphPad Software Inc., La Jolla, CA, USA) and SPSS 23.0 (IBM Analytics, UK) were used for statistical analyses. All data were checked for normality and homogeneity of variance using the Shapiro–Wilk and Levene tests, respectively. Data were presented as mean ± standard error. Differences among multiple comparisons were analyzed using two-way analysis of variance followed by Tukey's multiple comparison test. The difference between the two groups was assessed using student's *t* test (two-tailed). The body weight was analyzed using repeated measure ANOVA following Tukey's multiple comparison test. For data analysis that did not meet the normality and homogeneity of variance tests, nonparametric tests were used. The 16S rRNA gene sequencing data of the two groups were analyzed by the Wilcoxon rank-sum test. Spearman's correlation analyses were performed for the relative abundance of microbiota and inflammatory indicators or neurotransmitters. $P < 0.05$ was considered statistically significant.

3. Results

3.1 Physiological parameters of mice in diverse groups

The results revealed that inulin controlled metabolic balance during the chronic course of SCZ, as indicated by the body weight (BW) gain and plasma CRP levels (Fig. 1a and b). Similar BWs were observed in all groups at the beginning of the study. After intraperitoneal injection of MK-801, the BW of the mice in the SCZ model group was dramatically decreased compared to the CON group ($p < 0.001$) from day 7 to day 14

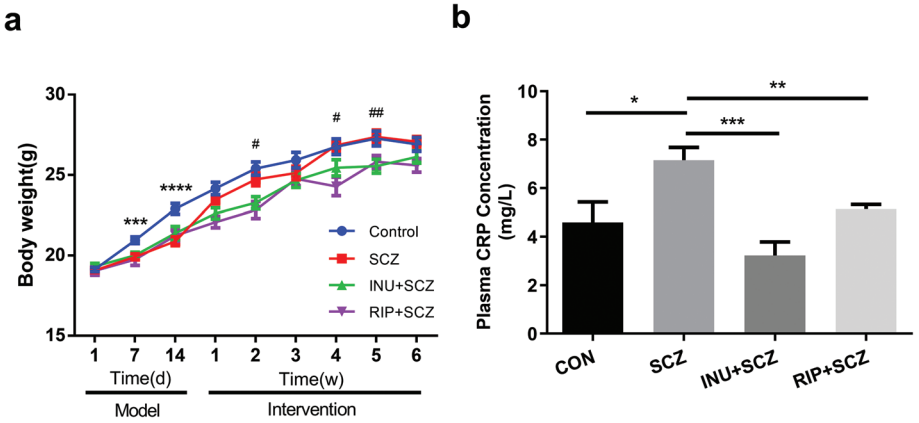

Fig. 1 Effects of diverse interventions on basic parameters of SCZ mice. (a) Changes in body weight (BW) in 14 days of MK-801 modelling and 6 weeks of different interventions; (b) plasma C-reactive protein (CRP) level. Data are presented as mean ± SEM. *$p < 0.05$, **$p < 0.01$, ***$p < 0.001$. In figure a, *: SCZ *vs.* CON; #: SCZ *vs.* INU + SCZ, using repeated measure ANOVA following Tukey's multiple comparison test.

during modelling, but there was no significant difference when compared to the CON group at the end of the experiment. Interestingly, during 6 weeks of drinking water intervention after modelling, there were significant differences in the BW between the SCZ and INU + SCZ groups at week 2 ($p < 0.05$), week 4 ($p < 0.05$), and week 5 ($p < 0.01$), indicating that inulin intervention affected the BW in SCZ mice. In addition, the BW of the RIP + SCZ and SCZ groups differed at week 4 of treatment ($p < 0.001$). Similar to the BW gaining process, the plasma CRP level was significantly increased in the SCZ group compared to the CON group ($p < 0.05$), INU + SCZ group ($p < 0.001$) and RIP + SCZ group ($p < 0.01$), respectively (Fig. 1b).

3.2 Inulin alleviated schizophrenia-like symptoms in mice

The behavioural tests were performed for 24 h after 6 weeks of drinking water intervention, including OFT (Fig. 2a) and MWM (Fig. 2g). Data from the two independent trials of behavioural testing were consistent with each other. In the OFT, the SCZ mice showed hypoactivity, including less total travelled distance (Fig. 2a and e), less rearing (Fig. 2c), and more travel in the exposed central region away from the walls (Fig. 2d and f), suggesting decreased exploratory behaviours and increased depressive-like behaviours. Promisingly, the number of rearing and total distance in SCZ mice were significantly increased after inulin intervention compared to the model group, indicating that inulin could alleviate SCZ-like symptoms in mice. Notably, the increasing trend of defecation was observed in the INU + SCZ group compared to the SCZ group (Fig. 2b), which further revealed that inulin may regulate anxiety and depression. However, after intervention with risperidone, the above indicators only showed an improvement trend without any significant differences when compared with the SCZ group.

Cognitive behaviours were also measured using the MWM test. In the positioning cruise experiment test (Fig. 2g and h), the SCZ mice took a significantly longer time to locate the escape platform than the CON group mice, indicating impaired learning memory. In the INU + SCZ and RIP + SCZ groups, the mice located the platform much faster than the mice in the SCZ group (Fig. 2h). Furthermore, in the space exploration experiment (Fig. 2i), mice in the SCZ group crossed the platform considerably less number of times than the CON group, suggesting impaired spatial recognition memory. Meanwhile, there was an increase in the number of times the INU + SCZ mice crossed the platform compared to the SCZ mice but the difference was not statistically significant. There was a decrease in the number of times the RIP + SCZ mice crossed the platform compared to the SCZ mice but without any significant difference.

Collectively, these behavioural tests demonstrated that the SCZ mice displayed locomotor hypoactivity, anxiety disorders and depressive-like behaviors, and impaired learning and spatial recognition memory, as they showed a longer latency to locate the escape platform during the training sessions and spent less time in the target quadrant in the MWM test compared to the others. However, after 6 weeks of inulin intervention, the above indicators have been improved, suggesting that inulin may be considered to regulate the intestinal microbiota through the MGB axis by affecting the transmission of brain synapses and issuing different behavioural instructions, thereby improving the abnormal behaviours of SCZ mice.

3.3 Inulin improved the brain physiology and pathomorphology of mice with schizophrenia

The brain BDNF levels in the SCZ group were notably decreased compared to the CON ($p < 0.001$), INU + SCZ ($p < 0.05$), and RIP + SCZ groups ($p < 0.01$) (Fig. 7d). The levels of neurotransmitter DA in the SCZ group were significantly higher than those in the CON group ($p < 0.01$) and RIP + SCZ group ($p < 0.05$), but showed no significant difference in the INU + SCZ group ($p > 0.05$) (Fig. 7e). Similarly, the brain 5-HT concentrations in the SCZ group were notably higher than those in the INU + SCZ group ($p < 0.001$) (Fig. 7f), but there was no significant difference between the SCZ and CON groups.

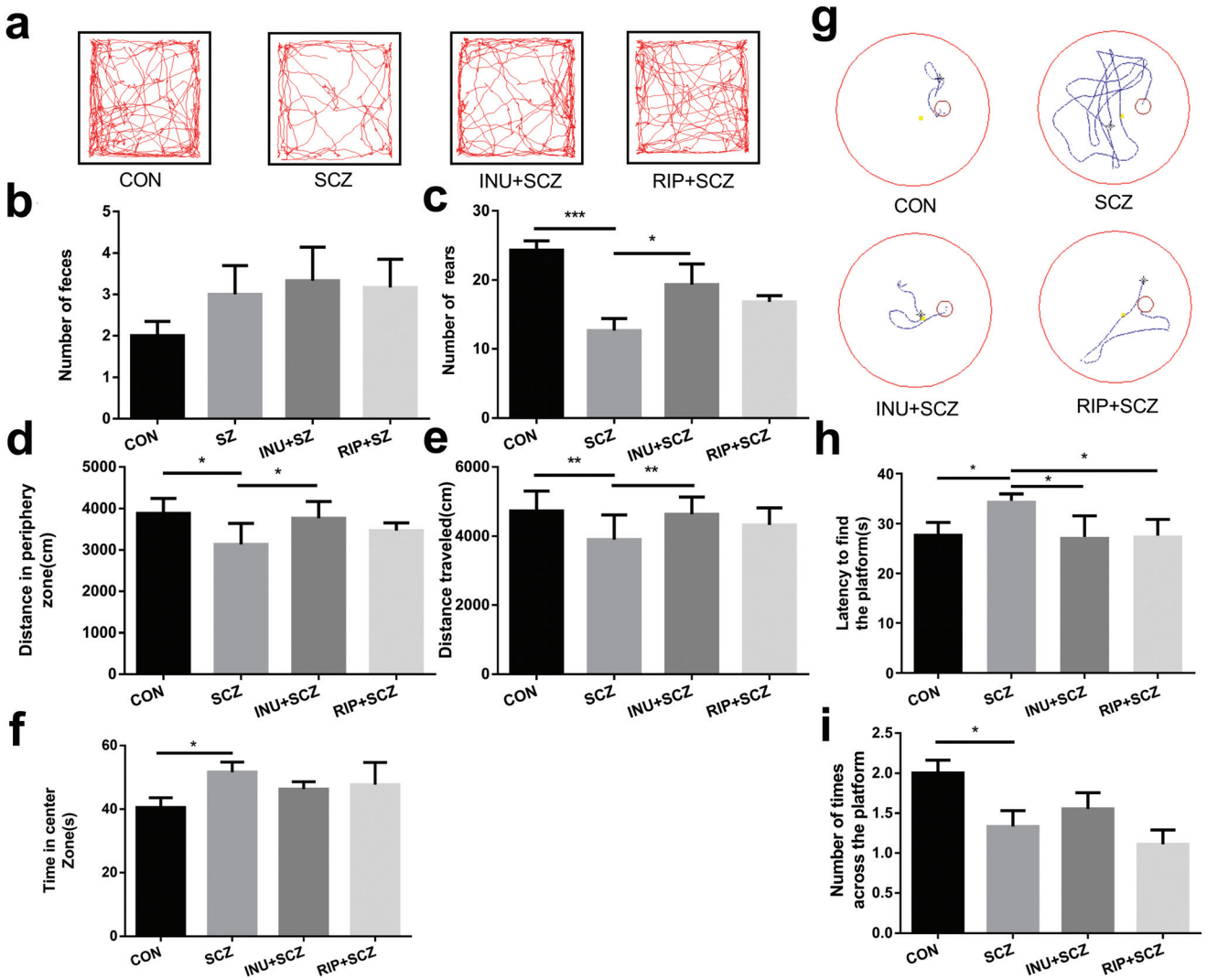

Fig. 2 Hypokinetic behaviour, impaired learning and memory in SCZ mice, and the reversal after inulin intervention. (a–f) Open field test (OFT), (g–i) Morris water maze (MWM). (a) An open field trajectory diagram for behavioural testing; (b) the number of faeces; (c) the number of rearing events; (d) the distance traveled in the peripheral zone (cm); (e) the cumulative distance traveled (cm); (f) the time in the central zone (s); (g) the representative traces of mouse activity in the MWM test; (h) the primary latency to find the platform within the 60 s training task of MWM along with 4 trails; (i) the number of times passing through the platform in the opposite quadrant during the 60 s probe test of recognition memory. All data were presented as mean ± SEM. *$p < 0.05$, **$p < 0.01$, ***$p < 0.001$.

To further confirm the pathological changes in the brain, HE staining, Nissl staining, and immunohistochemistry were performed respectively. First, HE staining showed that the hyperchromatic inflammatory cells were increased in the SCZ group compared to the CON group, whereas 6 weeks of inulin intervention distinctly alleviated the brain histopathological injury, and a similar result was found in the RIP + SCZ group (Fig. S1†). Moreover, the Nissl staining revealed that the SCZ group showed the loss and necrosis of neurons with light cell staining and nuclear condensation with deep staining in the various regions of the hippocampus (CA1, CA3, and DG) in contrast to that in the CON group (Fig. 3). When treated with inulin, the phenomenon of nuclear hyperchromatism was reduced compared to the SCZ group, suggesting that neuronal necrosis was alleviated.

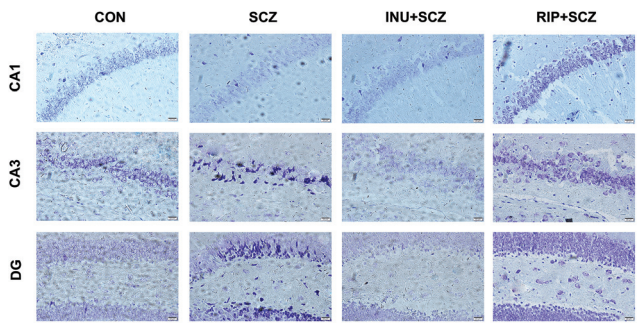

Fig. 3 Inulin ameliorated neuronal necrosis in SCZ mice. Nissl staining of the hippocampal regions CA1, CA3 and DG; bar = 20 μm.

It is worth noting that in this experiment the prebiotics directly affected the intestine and regulated the CNS. To test whether the effects were attributed to inflammation and the gut microbiota, the following experiments were performed.

3.4 Inulin significantly reduced chronic inflammation in mice with schizophrenia

First, in the immunohistochemistry of the prefrontal cortex of the brain, the microglia marker Iba-1 displayed a brown colour (Fig. 4a). The expression of Iba-1 in the SCZ group was found to be higher than that in the CON group using a 20× microscope objective lens, while the expression of positive cells in the INU + SCZ group was lower than that in the SCZ group. Using a 400× magnification to enlarge the local image of the corresponding area, it was found that the number of microglial cells was increased and the morphology was altered in the SCZ group compared to the CON group. The cells became larger with increased synaptic branches, indicating that the microglial cells were activated in the SCZ group. After inulin administration, the number of microglial cells was decreased, and the morphology was changed between the active and resting states. Similar results were found in the RIP + SCZ group. The statistical analysis of the proportion of the area occupied by positive cells showed that the positive cells in the SCZ group were significantly increased compared to the CON group ($p < 0.001$, Fig. 4b), while those in the INU + SCZ group or RIP + SCZ group were significantly decreased compared to the SCZ group ($p < 0.01$ and $p < 0.001$, respectively) (Fig. 4b).

Similarly, in the Iba-1 immunohistochemical staining of the hippocampus, consistent results were observed for the different regions (CA1, CA3, and DG), which further clarify the microglial expression under physiological, pathological, and interventional conditions in different parts of the brain (Fig. 5a and b). In the hippocampal CA1, CA3, and DG areas, the number of microglial cells in the SCZ group was significantly higher than that in the CON group (Fig. 5b–e). In the CA1 and CA3 areas, the number of positive cells in the INU + SCZ group was significantly lower than that in the SCZ group ($p < 0.01$ and $p < 0.05$, respectively), which was consistent with the results of the RIP + SCZ group (Fig. 5c and d). In the DG area, the relative number of microglial cells in the INU + SCZ group or the RIP + SCZ group was also decreased compared to the SCZ group, but the decrease was not statistically significant (Fig. 5e). These results indicated that excessive proliferation and activation of microglial cells in the SCZ group was clearly observed from the morphology, which could be reversed by inulin intervention.

To further assess the effects of inulin on the proportions of microglial activation and resting in SCZ mice, the microglial cells were analyzed using flow cytometry. The activated microglial cells were labeled with APC-CD11b^{+} and PE-CD45^{high+}, whereas the resting microglial cells were marked with APC-CD11b^{+} and PE-CD45^{+} (Fig. 6a). The results showed that the proportions of activated microglial cells and resting microglial cells were increased in the SCZ group compared to the CON group ($p < 0.001$) (Fig. 6b). Treatment with inulin decreased the proportions of activated and resting microglial cells compared to the SCZ group ($p < 0.001$) (Fig. 6b). Similar effects were observed for treatment with risperidone ($p < 0.001$).

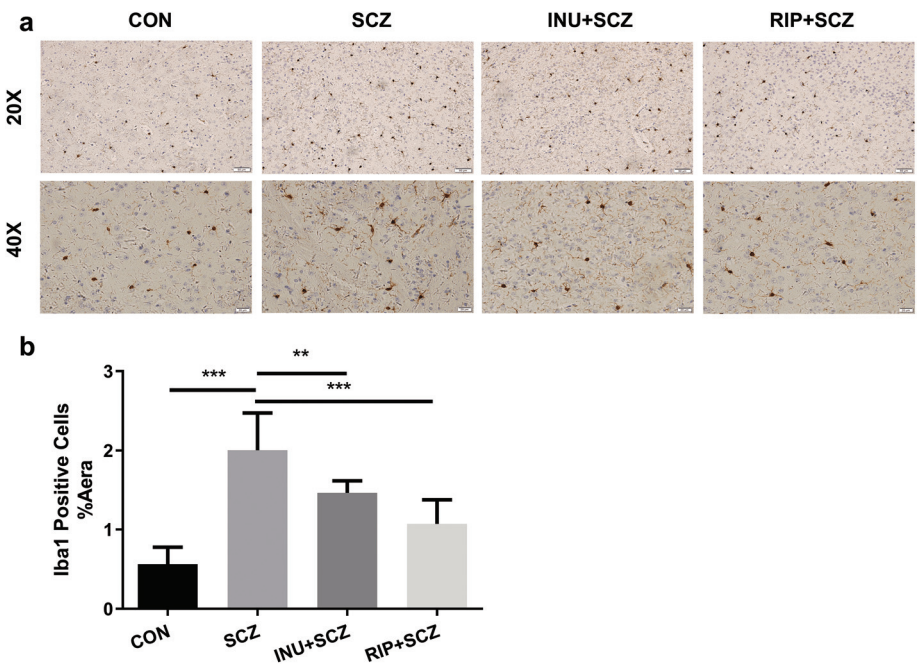

Fig. 4 Inulin significantly decreased the positive expression of brain Iba-1 in SCZ mice. (a) Results of microglial cell immunohistochemistry (IHC) in the brain prefrontal cortex. 20X Bar = 50 μm; 40X Bar = 20 μm. (b)The relative number of microglial Iba-1 cells in the prefrontal cortex of diverse groups. *$p < 0.05$, **$p < 0.01$, ***$p < 0.001$. All experiments were performed in triplicate.

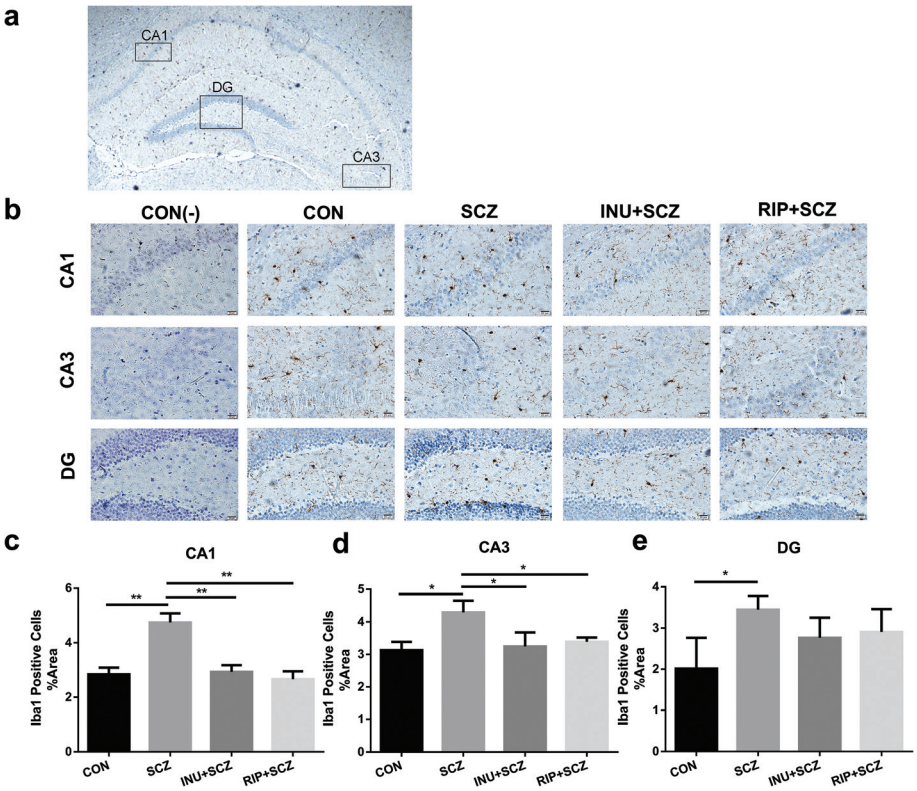

Fig. 5 Inulin notably decreased the microglial expression in different regions (CA1, CA3 and DG) of the hippocampus in SCZ mice. (a) The visual map of the hippocampus showing the corresponding observation parts. (b) Immunohistochemistry (IHC) of Iba1 in the hippocampus. Bar = 20 μm. (c–e) The relative number of microglial Iba-1 cells in the hippocampal regions CA1, CA3 and DG of diverse groups. *$p < 0.05$, **$p < 0.01$.

Parallel to the activation of microglial cells, the immune inflammatory indicators were also altered accordingly. After 6 weeks of intervention, inflammatory cytokines and bacterial endotoxins in the brain tissues and peripheral blood plasma were respectively measured. The results showed that TNF-α, IL-1β, IL-6 and IL-10 concentrations in the brain tissues were drastically higher in the SCZ group than in the CON group (all $p < 0.0001$) (Fig. 7a). As expected, these markers in the INU + SCZ or RIP + SCZ group were dramatically lower than those in the SCZ group (all $p < 0.01$). Plasma inflammatory cytokine concentrations also showed similar trends (Fig. 7b).

Moreover, the plasma concentration of LPS in the INU + SCZ group was significantly lower than that in the SCZ group ($p < 0.05$) but still higher than that in the CON group. This was similar to the RIP + SCZ group *versus* SCZ group results (Fig. 7c), suggesting that the effectiveness of inulin in the SCZ group might be related to the reduction of translocated LPS-induced endotoxaemia.

3.5 Inulin improved intestinal integrity and permeability

Based on the results of HE staining in diverse groups, the morphology of intestinal villi in the SCZ group were found to be shorter and incomplete compared to the CON group (Fig. S2a†). The intestinal mucosa became thinner and the cells were loosely arranged, suggesting that chronic inflammation caused pathological changes in the intestinal structure and function. However, these pathological changes improved after inulin treatment (Fig. S2a†). The length of the villi in the intestinal cavity could be used as an indirect indicator to evaluate the permeability of the intestinal mucosa. The measurement results showed that the length of the intestinal villi of the SCZ group was notably lower than that of the CON group ($p < 0.001$), and the length was dramatically increased after inulin or risperidone intervention ($p < 0.0001$, $p < 0.05$), especially in the INU + SCZ group (Fig. S2b†).

Immunohistochemistry analysis of the small intestine in the SCZ group showed that the positive cell staining was shallower than that in the CON group. After inulin intervention, the staining became significantly thicker, and a similar effect was observed in the RIP + SCZ group (Fig. 8a). Further statistical analysis revealed that ZO-1 and occludin were notably decreased in the SCZ group when compared with the CON group ($p < 0.001$ and $p < 0.05$, respectively). In the INU + SCZ group, the levels of ZO-1 and occludin were drastically increased compared to the SCZ group (both $p < 0.05$) (Fig. 8b and c).

3.6 Inulin modulated the gut microbiota in mice with schizophrenia

To further investigate the distinction in the gut microbiota of the SCZ mice treated with inulin, 16S rRNA sequencing and analysis were performed to measure 20 faecal samples

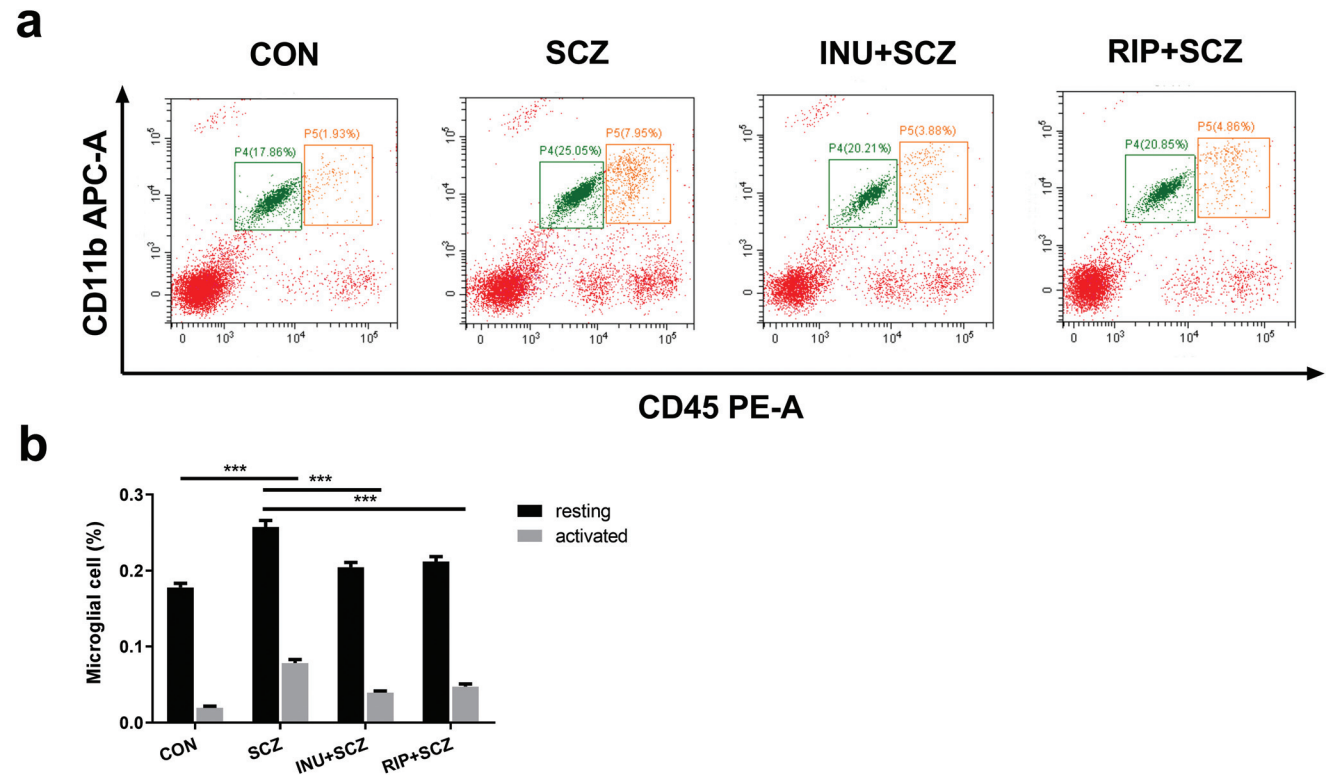

Fig. 6 Inulin significantly reduced inflammation in SCZ mice, including inhibition of excessive activation and an increase in the number of microglial cells. (a) Flow cytometry analysis of microglia $CD11b^{+}CD45^{+}$ cells and $CD11b^{+}CD45^{high+}$ cells in diverse groups. (b) The proportions of $CD11b^{+}CD45^{+}$ cells (resting microglia) and $CD11b^{+}CD45^{high+}$ cells (activated microglia). $^{**}p < 0.01$, $^{***}p < 0.001$.

obtained from the mice of the SCZ, INU + SCZ, RIP + SCZ, and CON groups. Strains with different abundances in different groups were used to evaluate the possible alterations in function and correlations with indicators including behaviours, neurotransmitters, inflammatory factors and pathomorphology. We obtained 1 422 459 high-quality sequences across all samples with an average length of 421.55 base pairs. Taxonomic composition at the species level was characterised by operational taxonomic units (OTUs). A Venn diagram showed that 94 of 479 OTUs were commonly detected in the four groups, while 5, 1, 3 and 6 OTUs were unique in the SCZ, INU + SCZ, RIP + SCZ, and CON mice, respectively (Fig. 9a). Most rarefaction curves tended to approach the saturation plateau, suggesting that the sequencing depth was reasonable and sufficient to cover the entire bacterial diversity (Fig. S3b†).

To determine whether the microbial composition of SCZ mice with various interventions differed substantially from that of the CON group mice, we performed β-diversity analysis. This analysis revealed that principal coordinate analysis (PCoA) of OTUs at the phylum and genus levels corroborated the distinction among the four groups (Fig. 9b and c), but there were still crossovers among individual sample points, for eliminating the intragroup differences and comparing the inter-group differences, partial least squares discriminant analysis (PLS-DA) was performed with the classical partial least squares regression model. Significant discrimination was observed among the four groups at the phylum and genus levels, indicating that there were distinctive species in each group (Fig. 9d and e).

At the phylum level, the proportion of *Firmicutes* was lower in the SCZ group than in the other three groups, but there was no statistical difference (Fig. 10a). The relative abundances of *Proteobacteria* and *Patescibacteria* in the SCZ group were significantly lower than those in the CON group ($p = 0.0278$ and $p = 0.02157$, respectively) (Fig. 10c), which were reversed by RIP treatment ($p = 0.03671$ and $p = 0.0278$, respectively) (Fig. 10e). Meanwhile, the proportion of *Verrucomicrobia* was significantly higher in the SCZ group than that in the CON group ($p = 0.01219$), INU + SCZ group ($p = 0.02157$) and RIP + SCZ group ($p = 0.01219$) (Fig. 10c, e and g). Intriguingly, after inulin administration, the abundance of *Actinobacteria* was dramatically increased in the INU + SCZ group compared with the SCZ group ($p = 0.02157$) (Fig. 10e). Collectively, our data revealed that inulin intervention had a major effect of increasing *Actinobacteria* and decreasing *Verrucomicrobia* in the INU + SCZ group but limited effects on *Bacteroidetes* and *Firmicutes* (Fig. 10a).

To further understand the effects of inulin on the composition of the gut microbiota in SCZ, the microorganisms at the genus level were investigated (Fig. 10b). We found that *Desulfovibrio*, *Alistipes*, *unclassified f-Lachnospiraceae*, *Lachnoclostridium*, and *Muribaculum* were the most prevalent

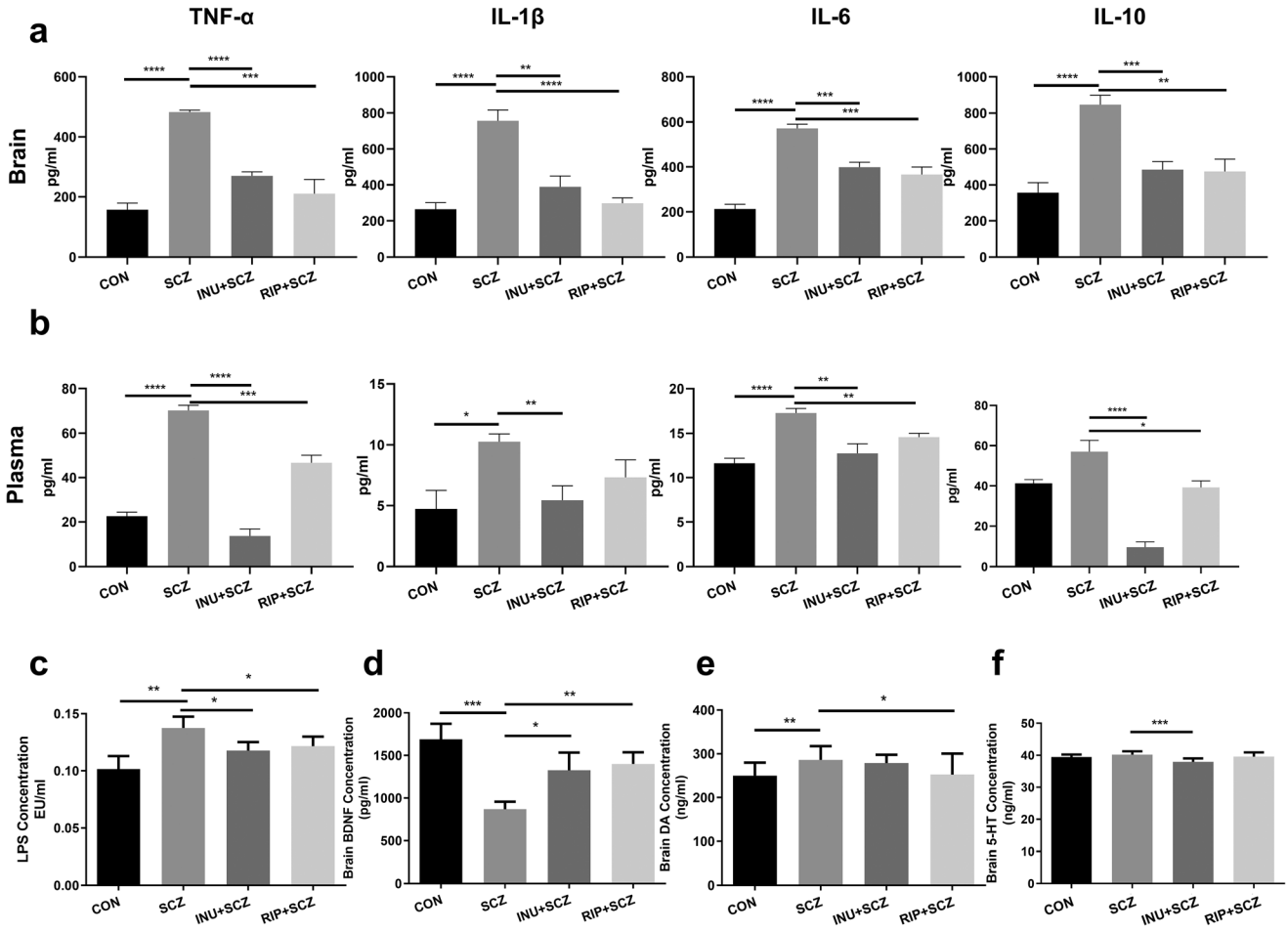

Fig. 7 Effects of inulin on inflammatory cytokines, neurotransmitters and lipopolysaccharide (LPS) levels in diverse groups. The supernatants of brain tissue or plasma were collected to determine the concentrations of TNF-α, IL-1β, IL-6, and IL-10 by using ELISA kits and the LPS levels with a limulus amebocyte lysate kit. (a) The concentrations of TNF-α, IL-1β, IL-6 and IL-10 in brain tissues. (b) The concentrations of TNF-α, IL-1β, IL-6 and IL-10 in plasma. (c) The concentration of plasma LPS. The supernatants of the brain tissue were collected for detection of BDNF (d), DA (e) and 5-HT (f) levels using ELISA kits, respectively. Data are presented as mean ± SEM. *$p < 0.05$, **$p < 0.01$, ***$p < 0.001$, ****$p < 0.0001$. All experiments were performed in triplicate. TNF-α: tumour necrosis factor-α; IL-6: interleukin-6; IL-1β: interleukin-1β; IL-10: interleukin-10; LPS: lipopolysaccharide; BDNF: brain-derived neurotrophic factor; 5-HT: 5-hydroxytryptamine; and DA: dopamine.

genera in the CON group and they were obviously reduced in the SCZ group ($p < 0.05$) (Fig. 10d). While the proportions of *Akkermansia* and *Eubacterium-fissicatena* were dramatically higher in the SCZ group than those in the other three groups ($p < 0.05$) (Fig. 10d and f). Moreover, the abundance of *Lactobacillus* in the INU + SCZ group was higher than that in the SCZ group, but without statistically significant difference ($p = 0.1437$). *Bifidobacterium* was sharply elevated in the INU + SCZ group compared with the SCZ group ($p = 0.03615$) (Fig. 10f). The proportion of *Desulfovibrio* was significantly reduced in the SCZ group compared to the CON group ($p = 0.03219$) (Fig. 10d), which was reversed by RIP treatment ($p = 0.02157$) (Fig. 10h). In addition, *Bacteroides* and *Marvinbryantla* were dramatically higher in the RIP + SCZ group than those in the SCZ group ($p = 0.01219$ and $p = 0.03671$, respectively) (Fig. 10h). Overall, the genus results showed that the chronic process of SCZ changed the initial proportion of OTUs, mainly including *unclassified f-Lachnospiraceae*, *Desulfovibrio*, *Lachnoclostridium*, *Alistipes*, *Muribaculum*, *Akkermansia*, and *Eubacterium-fissicatena*. Dietary inulin restored the gut dysbiosis by increasing *Bifidobacterium* and *Lactobacillus* and decreasing *Akkermansia* and *Eubacterium-fissicatena*. Furthermore, the heat map also showed similar results (Fig. S3a†).

3.7 Altered gut microbes in mice with schizophrenia and their association with neurotransmitters and inflammatory cytokines

Among the top 30 species ranging from high to low microbial abundance, Spearman's correlation was used to analyze the correlation between explicit species and specific neurotransmitters or inflammatory cytokines. First, Spearman's correlation analysis showed that the change in the 5-HT level in the brain tissue was positively associated with *Parasutterella* ($r = 0.6033$, $p < 0.01$), *Blautia* ($r = 0.5568$, $p < 0.05$), *Parabacteroides* ($r = 0.5043$, $p < 0.05$), and *Eubacterium-fissicatena* ($r = 0.4934$, $p < 0.05$) but negatively associated with *Lactobacillus* ($r =$

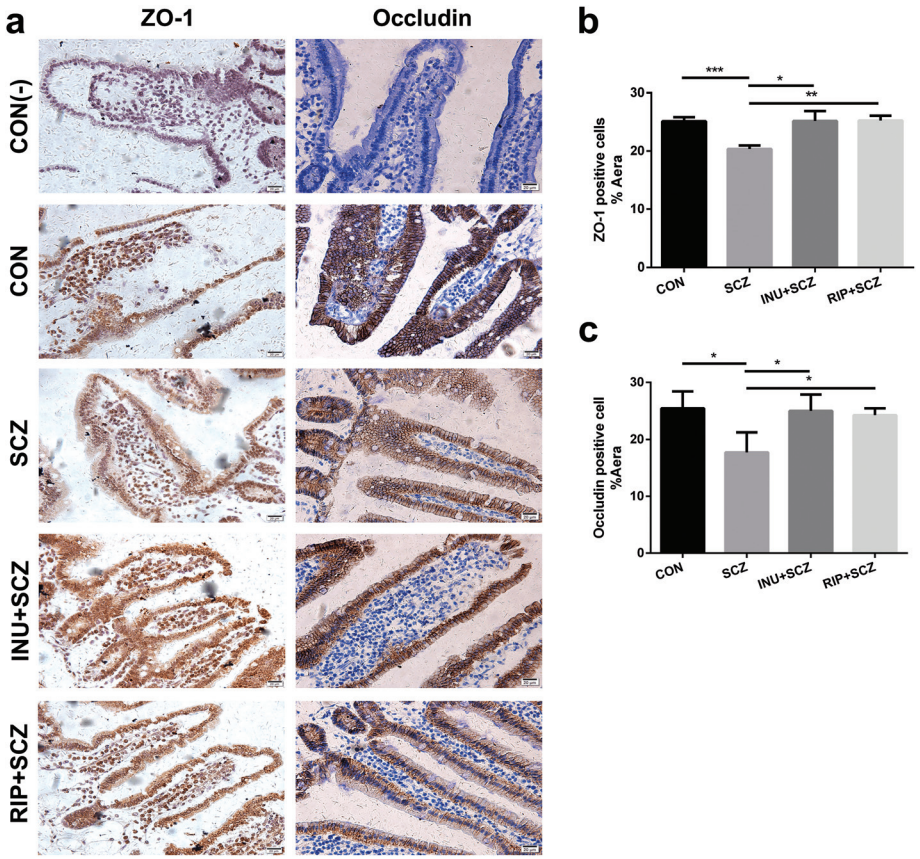

Fig. 8 Inulin significantly changed the positive expression of ZO-1 and occludin in the small intestine of SCZ mice. (a) Small intestine immunohistochemistry (IHC) was performed using rabbit anti-mouse ZO-1 antibody and rabbit anti-mouse occludin antibody, respectively. Bar = 20 μm. (b) The positive expression of ZO-1 cells in diverse groups. (c) The positive expression of occludin cells in diverse groups. *$p < 0.05$, **$p < 0.01$, ***$p < 0.001$. All experiments were performed in triplicate.

−0.5664, $p < 0.01$), *Muribaculum* ($r = -0.5461$, $p < 0.05$), *Alistipes* ($r = -0.5290$, $p < 0.05$), *Turicibacter* ($r = -0.4927$, $p < 0.05$), *Lachnospiraceae-NK4A136* ($r = -0.4874$, $p < 0.05$), and *Bifidobacterium* ($r = -0.4582$, $p < 0.05$). The DA level in the brain tissue was negatively associated with *unclassified-f-Ruminococcaceae* ($r = -0.4479$, $p < 0.05$). Moreover, BDNF in the brain tissue was positively associated with *Alistipes*, *Muribaculum*, *Lachnoclostridium*, and *norank-f-Lachnospiraceae* ($r = 0.4612$, $r = 0.4889$, $r = 0.4962$ and $r = 0.4507$, respectively; all $p < 0.05$) but negatively associated with *Akkermansia* ($r = -0.7100$, $p < 0.001$) and *Parabacteroides* ($r = -0.4543$, $p < 0.05$) (Fig. 11a, Table S1†).

Next, the correlation between faecal microbial species abundance and brain inflammatory concentrations was identified (Fig. 11b, Table S2†). In brief, the abundance of *Akkermansia* was found to be positively associated with the brain levels of TNF-α ($r = 0.6732$, $p < 0.01$), IL-1β ($r = 0.5639$, $p < 0.01$), IL-6 ($r = 0.7113$, $p < 0.001$), and IL-10 ($r = 0.7281$, $p < 0.001$). In addition, the abundances of *Dubosiella* and *Parasutterella* were positively associated with IL-1β ($r = 0.4722$ and $r = 0.4605$, respectively; both $p < 0.05$). The abundance of *Parabacteroides* was positively associated with IL-10 ($r = 0.4686$, $p < 0.05$). In contrast, among the 10 microbial species with significant negative correlation with the above inflammatory cytokines, *Alistipes* showed the highest correlation with TNF-α, IL-1β, IL-6, and IL-10 ($r = -0.7446$, $r = -0.7537$, $r = -0.7514$, and $r = -0.6810$, respectively), followed by *Lachnoclostridium* and *Ruminiclostridium*.

4. Discussion

In the present study, we investigated the efficacy of dietary inulin administration in mice with SCZ. After 6 weeks of treatment, the results demonstrated that inulin alleviated the damage of brain neurons. The beneficial effects could be due to the suppression of the over-activated microglial cells by inhibiting the release of inflammatory indicators and modulating the gut microbiota. This intervention caused fewer side effects and showed higher preventive and therapeutic potential than the other modalities, probably due to the MGB axis involvement. The following discussion is regarding the MGB axis from the perspective of microorganisms to explore how inulin in SCZ model mice improves the damaged intestinal mucosal barrier by regulating the gut microbiota to reduce LPS translocation into the circulatory system to inhibit inflammation. The

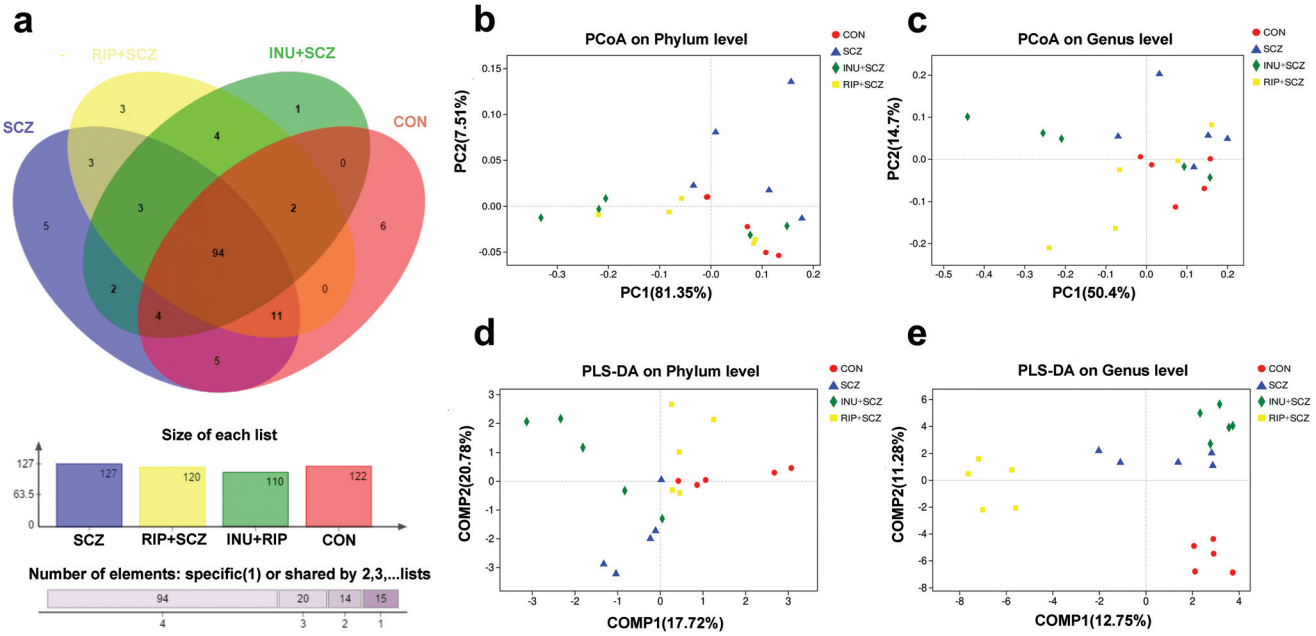

Fig. 9 Altered gut microbiome in each group of mice. (a) Venn diagram of microbial species number in the faeces of diverse groups. The microbial species with different abundance among diverse groups including SCZ mice (purple circle), CON mice (red circle), INU + SCZ mice (green circle) and RIP + SCZ mice (yellow circle). (b) and (c) Principal coordinate analysis (PCoA) score plots based on the Bray–Curtis distance at the phylum and genus levels for microbiome in the faeces, respectively. (d) and (e) Partial least squares discriminant analysis (PLS-DA) score plots at the phylum and genus levels for microbiome, respectively (n = 5 per group).

cascade effect, which in turn reduces the activation of microglia in the CNS, ultimately leads to partial reversal of neuronal damage and effective relief of SCZ-like symptoms.

In this study, the gut microbiota was significantly altered in the INU + SCZ group compared to the SCZ group. Growing evidence has demonstrated that gut dysbiosis is closely associated with the onset and progression of SCZ.[31,32] The microbial sequencing results of our study showed that *Bacteriodetes* and *Firmicutes* were the most dominant in all four groups at the phylum level, which was consistent with previous human and animal studies,[33–35] whereas there were no significant differences in the abundance among the diverse groups. Decreased *Proteobacteria* and *Patescibacteria* and increased *Verrucomicrobia* in our results were responsible for gut dysbiosis in SCZ. More importantly, the abundance of *Actinobacteria* was notably increased in the INU + SCZ group compared with the SCZ group, which was in agreement with previous studies on humans and animals.[36,37] This revealed that supplementary inulin might modulate gut dysbiosis in SCZ mice by increasing the gut *Actinobacteria*. *Actinobacteria*, Gram-positive microorganisms, are mainly aerobes with an oxidative metabolism, but several species are facultative anaerobes or even strict anaerobes. In addition, *Actinobacteria* are able to metabolize amino acids, and some strains can degrade aromatic hydrocarbons. They are major producers of medically important antibiotics as they are members of the genus *Streptomyces*, the most abundant group of *Actinobacteria.*[38]

At the genus level, the results also revealed that inulin could restore gut dysbiosis in SCZ by upregulating beneficial bacteria (*Bifidobacterium* and *Lactobacillus*),[24,39] especially *Bifidobacterium*, and downregulating probable pathogenic bacteria such as *Akkermansia*, which are mucin-degrading bacteria that reside in the mucus layer. *Bifidobacterium* is thought to promote health and restore mucus growth by producing antimicrobial substances that protect the host from opportunistic pathogens.[40,41] Therefore, it was suspected that the improvement in the intestinal environment by increasing the abundance of *Bifidobacterium* might be beneficial for the maintenance and promotion of a healthy condition.[42] *Lactobacillus*, a genus of commensal bacteria existing as microaerophiles or facultative anaerobes, affects the intestinal integrity by producing a ligand of the aryl hydrocarbon receptor (AhR), indole-3-aldehyde, that contributes to AhR-dependent IL-22 transcription and mucosal protection from inflammation.[43] The colonisation of *Akkermansia* in the intestine is closely related to the host health. The genus *Akkermansia* is known to be effective in improving gut barrier function by increasing the thickness of the intestinal mucus layer, resulting in a beneficial immune response. Emerging evidence also reveals that the abundance of *Akkermansia* has an inverse correlation with the consequences of inflammation, such as obesity, T2DM, and non-alcoholic fatty liver disease.[44,45] Despite of showing beneficial effects in most cases, there are still some contradictory reports. For instance, a recent study has shown that Parkinson's disease was associated with increased intestinal *Akkermansia* genera,[46] and deprivation of dietary fibers caused *Akkermansia* to erode the mucus layer,[47] which was consistent with our findings. Our study found that the pathological

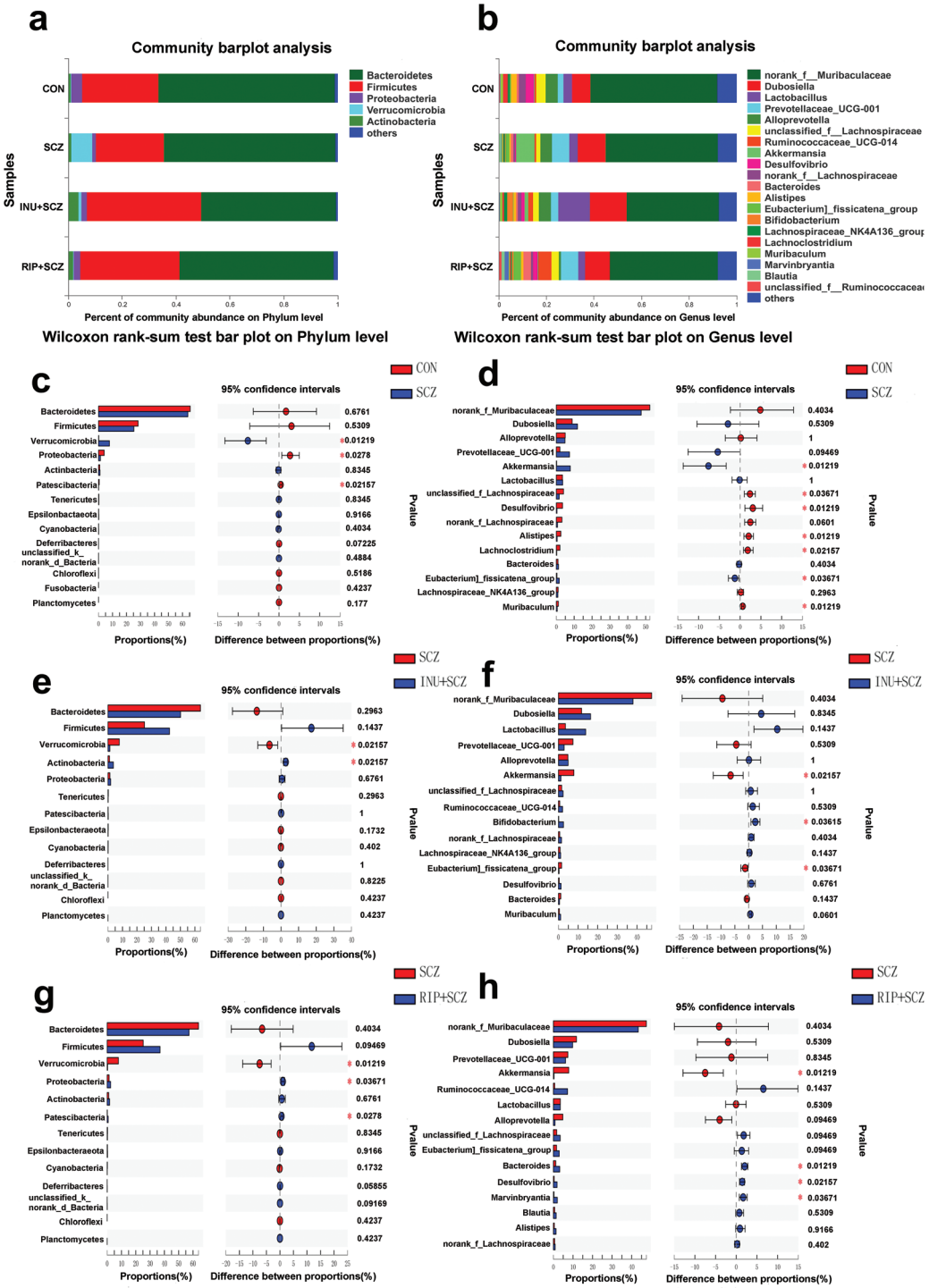

Fig. 10 Relative abundance of microbial species at the phylum and genus levels in the faeces of mice. (a) Community abundance at the phylum level. (b) Community abundance at the genus level. (c), (e) and (g) The phylum analysis of CON *vs.* SCZ, SCZ *vs.* INU + SCZ, and SCZ *vs.* RIP + SCZ, respectively. (d), (f) and (h) The genus analysis of CON *vs.* SCZ, SCZ *vs.* INU + SCZ, and SCZ *vs.* RIP + SCZ, respectively. *$p < 0.05$, ($n = 5$ per group).

process of SCZ seemed to be closely related to the increase in *Akkermansia*. However, after inulin intervention, the abundance of *Akkermansia* was significantly decreased, while those of *Bifidobacterium* and *Lactobacillus* were increased. Furthermore, the levels of inflammatory cytokines, including TNF-α, IL-1β, IL-6, and IL-10, positively associated with *Akkermansia* were also decreased. This showed that inulin could improve the intestinal microenvironment by changing the abundance of the gut microbiota and their metabolites, thereby exerting a protective effect on the intestinal mucosal barrier.

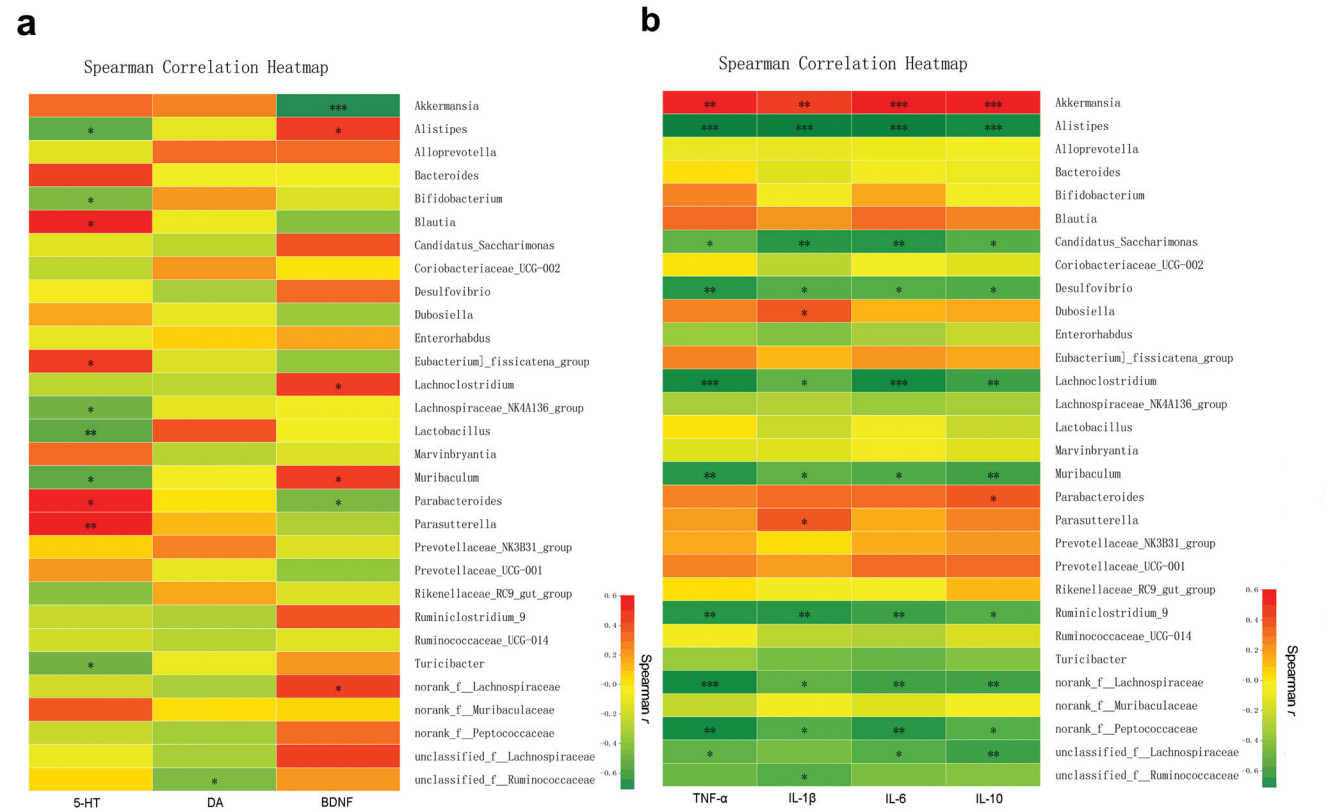

Fig. 11 Correlation of microbial abundance with neurotransmitters and inflammatory cytokines at the genus level. (a) The heat map showing the correlation of different microbial abundance with neurotransmitters and BDNF. (b) The heat map showing the correlation of different microbial abundance with inflammatory cytokines in the brain tissue. The intensity of the colour indicates the degree of correlation between the corresponding factor and each microbial species, which was obtained by Spearman's correlation analysis. *p < 0.05, **p < 0.01, ***p < 0.001, (n = 5 per group).

Furthermore, the intestinal mucosal barrier formed by intestinal epithelial cells and intercellular connections is an important defence barrier that prevents pathogenic microorganisms and their metabolites from penetrating the intestine and entering the blood.[48] Tight junction indicators, ZO-1 and occludin, play indispensable roles in maintaining the intestinal mucosal barrier.[49] Our morphological results showed that the expression levels of the tight junction proteins (occludin and ZO-1) were reduced in SCZ mice, indicating increased intestinal permeability and impaired mucosal barrier, which were also observed in other diseases, such as in celiac disease,[50] IBD,[51] and diabetes.[52] However, drastically elevated expression of ZO-1 and occludin in the INU + SCZ group suggested that inulin could improve intestinal integrity and permeability, which was consistent with a previous study.[39] In addition, Viorica Braniste *et al.*[53] reported that microbiota dysbiosis was associated with altered expression of tight junction proteins and increased blood–brain barrier permeability.

Furthermore, the reduction of LPS in plasma was noted in the INU + SCZ group, demonstrating that dietary inulin reduced gut permeability and LPS translocation from the intestine to the systematic circulation in the SCZ mice. LPS, a crucial trigger of inflammation, binds to the Toll-like receptor-4 (TLR-4) of antigen presenting cells, resulting in a cascade application reaction for the release of inflammatory cytokines through the leaky intestinal mucosal barrier that induces brain damage. Further analysis in this study showed that the reduction of the plasma or brain pro-inflammatory cytokines (TNF-α, IL-6, and IL-1β) and CRP levels after inulin treatment confirmed the suppression of the inflammatory response. These results were in agreement with the previous findings on the anti-inflammatory effects of inulin in chronic metabolic diseases.[20,25,54] Thus, the current results elucidated that inulin effectively alleviated endotoxemia and inflammation in SCZ.

This study documented neuroinflammation as a causative factor in SCZ. The increased levels of TNF-α activate nuclear factor-kappa B (NF-κB), which in turn promotes the production of the pro-inflammatory cytokines IL-6 and IL-1β, and the T-cell derived cytokine interferon gamma.[55] This may accelerate the generation and accumulation of free radicals and lipid peroxidation, activate microglial cells, and increase neuroexcitatory activity, ultimately leading to neurodegenerative effects.[56] It is well known that microglial cells are resident macrophages in the CNS with characteristic roles in combating infection, clearing cellular debris, and maintaining homeostasis, and involvement in complex neurodevelopmental programs such as neurogenesis and synaptic pruning.[57] In this study, the immunohistochemistry of microglia in the frontal

cortex and hippocampus demonstrated that inulin could effectively reverse the excessive activation of microglia and protect neurons from damage by reducing the release of inflammatory cytokines. The results of flow cytometry combined with immunohistochemistry of microglia further quantified the activation status of microglia and assessed the therapeutic effect after inulin intervention. Our results showed that TNF-α, IL-1β, and IL-6 levels in plasma and brain tissues in the INU + SCZ group were both significantly decreased, demonstrating that dietary inulin alleviated neuroinflammation mainly by reducing pro-inflammatory cytokines. Activation of microglial cells induces oxidative stress and produces pro-inflammatory cytokines TNF-α, IL-1β, and IL-6, causing degeneration of neurocytes and consequently resulting in excitotoxicity-induced neuronal death.[57] We also speculated that IL-10 could play a complicated role in the imbalance between the regulation of pro- and anti-inflammatory mediators during the chronic process of neuroinflammatory diseases, since IL-10 in this study differed from our previous study on ALD[25] in that it was decreased after inulin administration.

To evaluate the effects of inulin on the brain in SCZ mice, a series of brain physiological indicators (BDNF, 5-HT and DA) were analysed. BDNF, a neurotrophin playing essential roles in neurogenesis, is related to neuronal excitability, synaptic transmission, and maintenance of neuronal plasticity.[58,59] In addition, it has been documented that BDNF attenuates TNF-α and IL-1β by inhibiting NF-κB signalling.[60] In this study, the BDNF level in the SCZ group was notably decreased but was obviously increased in the INU + SCZ group. The current results were consistent with previous studies,[61,62] demonstrating that dietary inulin could increase neurogenesis in SCZ against neurodegeneration in the brain.

The concentrations of 5-HT and DA in the brains of the mice in each group were also measured to assess whether inulin changed the synthesis and release of neurotransmitters through the MGB axis. The gut microbiota catabolises food-derived tryptophan into a range of neuroactive catabolites,[55,63] such as kynurenine (Kyn), kynurenic acid (Kyna) and quinolinic acid (Quia), which can remotely affect the central glutamate and serotonin systems.[64,65] Moreover, the other two products of tryptophan metabolism are the ligands of AhR[43] and 5-HT.[66] The former is related to the integrity and permeability of the mucosal barrier, whereas the latter, a neurotransmitter related to mood, is synthesized in colon chromaffin cells and can be used as a potential mediator between the gut microbiota and brain pathophysiology. It has been reported that systemic inflammation induced by LPS caused the release of 5-HT in the hippocampus. After administration of prebiotics, the concentration of 5-HT was reduced, accompanied by decreases in the IL-1β and TNF-α levels,[67] which was consistent with the current experimental results. Furthermore, DA has been accepted as one of the main neurotransmitters that are disturbed in SCZ.[68] An elevated concentration of DA in our experiment corroborated with a previous study.[69] It is worth noting that after intervention with inulin, the results of a significant decrease in the concentration of 5-HT and no significant changes in the DA level revealed that inulin mainly regulated the production and release of 5-HT, but had no significant regulatory effect on the elevated DA concentration under the pathological conditions of SCZ. This further confirmed that the effect may be related to the tryptophan metabolism pathway of maintaining the homeostasis of normal synaptic function and neurotransmission in SCZ,[65,70] and the underlying mechanism needs to be further investigated.

Next, the correlation analysis between the gut microbiota and neurotransmitters or inflammatory indicators revealed that *Lactobacillus*, *Bifidobacterium*, *Muribaculum*, *Alistipes*, and *Lachnospiraceae NK4A136* were negatively correlated with 5-HT and proinflammatory cytokines, while *Alistipes*, *Muribaculum* and *Lachnospiraceae* were positively correlated with BDNF. In contrast, *Akkermansia* was negatively correlated with BDNF and positively correlated with inflammatory cytokines in the SCZ mice. Meanwhile, *Parasutterella*, *Parabacteroides*, and *Eubacterium fissicatena* were positively correlated with 5-HT. Interestingly, among these bacteria, *Parasutterella* was positively correlated with IL-1β, which was consistent with the study of Chen *et al.*[71] *Parabacteroides* was positively correlated with IL-10 and negatively correlated with BDNF. This was in agreement with the above results, further confirming that inulin alleviated SCZ by modulating the gut microbiota by increasing *Lactobacillus* and *Bifidobacterium* and decreasing *Akkermansia*, which triggered a series of related inflammatory and metabolic reactions. In this case, decreased concentrations of 5-HT correspondingly reduced the abundance of *Parasutterella*, *Parabacteroides*, and *Eubacterium fissicatena*, further contributing to an increase in BDNF and a decrease in inflammatory cytokines. Moreover, along with the tryptophan metabolic pathway, when both 5-HT and inflammatory cytokines were reduced, it may be inferred that the AhR could increase accordingly and may exert positive effects in improving the mucosal barrier function. In this situation, the tryptophan–kynurenine metabolism tended to be balanced, and neuroexcitatory toxicity and neurodegeneration were reversed.

To further validate the effect of inulin on the reversal of brain pathological changes, HE staining and Nissl staining were performed. HE and Nissl staining revealed that inulin dramatically ameliorated brain inflammatory cell infiltration and neuronal necrosis in SCZ mice. The brain morphological changes together with the above physiological indices indicated that inulin had a significant restorative effect on SCZ brain neuronal damage, further contributing to the mitigation of the SCZ-like symptoms. Memory impairment and hyperactivity are very common traits observed in the rodent models of SCZ.[72,73] However, in this study, we found that SCZ mice injected with *N*-methyl-D-aspartate (NMDA) receptor antagonist MK-801 for 14 consecutive days displayed behavioural abnormalities, including psychomotor hypoactivity and cognitive dysfunction. This phenomenon may be more biased towards the negative symptoms of SCZ due to the decline of glutamatergics caused by long-term administration of NMDA receptor antagonists. After administration of inulin, the abnormal behaviours (locomotor hypoactivity, anxiety disorders, depressive

behaviours, and impaired learning ability) were dramatically improved. These beneficial effects of inulin were similar to those elicited in the study by Kao *et al.*[74,75] which also showed the effects of the other prebiotic to alter NMDA receptors, attenuate metabolic dysfunction, and exert beneficial effects on depression and cognitive function in psychosis. The efficacy of inulin in SCZ mice showed no statistical change in spatial memory function, which was coincident with the limited efficacy of risperidone treatment of negative SCZ symptoms.[76,77] However, in view of the certain improvement trend, an entirely new treatment approach needs to be explored to overcome the limitations of the current antipsychotic medications.

In this study, we also found that the BW was lower in the SCZ group at the end of modelling,[78,79] but dietary inulin administration for 6 weeks effectively slowed the regain of BW in SCZ mice after modelling. This result was consistent with that of mice with diabetes or hyperlipidemia mice treated with inulin,[20,80] indicating that inulin can also regulate glucose and lipid metabolism, possibly by modulating intestinal microorganisms to improve body homeostasis. However, the exact mechanism of these bacterium candidates as well as their metabolites (SCFA, *etc.*) affecting the synthesis and release of neurotransmitters and inflammatory cytokines *via* the MGB axis is largely unknown. Further studies are required at the metagenomic and cellular levels to prove this pathological mechanism.

5. Conclusions

This study highlighted that dietary inulin ameliorated SCZ *via* modulation of the gut microbiota and anti-inflammation in mice, thus providing a theoretical foundation for future inulin intervention in the treatment of SCZ.

Abbreviations

SCZ	Schizophrenia
MGB axis	Microbiome–gut–brain axis
T2DM	Type 2 diabetes mellitus
IBD	Inflammatory bowel disease
SCFAs	Short chain fatty acids
ALD	Alcoholic liver disease
CNS	Central nervous system
RIP	Risperidone
OFT	Open-field test
MWM	Morris water maze
CRP	C-reactive protein
LPS	Lipopolysaccharide
5-HT	5-Hydroxytryptamine
DA	Dopamine
BDNF	Brain-derived neurotrophic factor
IL	Interleukin
TNF-α	Tumor necrosis factor-α
ELISA	Enzyme linked immunosorbent assay
INU	Inulin
HE	Hematoxylin and eosin
PCR	Polymerase chain reaction
BW	Body weight
OTUs	Operational taxonomic units
PCoA	Principal coordinate analysis
PLS-DA	Partial least squares discriminant analysis
NMDA	*N*-methyl-D-aspartate
Kyn	Kynurenine
Kyna	Kynurenic acid
Quia	Quinolinic acid
AhR	Aryl hydrocarbon receptor
TLR-4	Toll-like receptor-4
ZO-1	Zonula occludens 1.

Author contributions

Conceptualization: H. W., L. G. and J. L; methodology: PL. X., Y. Y., L. G., XX. Z., HX. L., M. Y and HY. T.; software: Y. Y.; validation: H. W., L. G., J. L. and PL. X.; data analysis: L. G., T. W., and Y. Y.; writing—original draft preparation: L. G. and PL. X.; writing—review and editing: H. W. and L. G.; supervision: J. L. and H. W.; project administration: H. W.; and funding acquisition: J. L. All authors have read and agreed to the published version of the manuscript.

Conflicts of interest

The authors declare that they have no competing interests.

Acknowledgements

This work was supported by the National Natural Science Foundation of China (Project No.: 82060238) and Ningxia High School first-class Disciplines (West China first-class Disciplines Basic Medical Sciences at Ningxia Medical University) (Project No.: NXYLXK2017B07). The authors thank Dr Kai Qi (Shanghai Applied Protein Technology Co., Ltd) for providing support.

References

1 J. Long, G. Huang, W. Liang, B. Liang, Q. Chen, J. Xie, J. Jiang and L. Su, The prevalence of schizophrenia in mainland China: evidence from epidemiological surveys, *Acta Psychiatr. Scand.*, 2014, **130**, 244–256, DOI: 10.1111/acps.12296.

2 M. Knapp, R. Mangalore and J. Simon, The global costs of schizophrenia, *Schizophr. Bull.*, 2004, **30**, 279–293, DOI: 10.1093/oxfordjournals.schbul.a007078.

3 H. A. Whiteford, L. Degenhardt, J. Rehm, A. J. Baxter, A. J. Ferrari, H. E. Erskine, F. J. Charlson, R. E. Norman, A. D. Flaxman, N. Johns, R. Burstein, C. J. Murray and

T. Vos, Global burden of disease attributable to mental and substance use disorders: findings from the Global Burden of Disease Study 2010, *Lancet*, 2013, **382**, 1575–1586, DOI: 10.1016/S0140-6736(13)61611-6.

4 M. G. Codagnone, S. Spichak, S. M. O'Mahony, O. F. O'Leary, G. Clarke, C. Stanton, T. G. Dinan and J. F. Cryan, Programming Bugs: Microbiota and the Developmental Origins of Brain Health and Disease, *Biol. Psychiatry*, 2019, **85**, 150–163, DOI: 10.1016/j.biopsych.2018.06.014.

5 T. V. Lipina, C. Zai, D. Hlousek, J. C. Roder and A. H. Wong, Maternal immune activation during gestation interacts with Disc1 point mutation to exacerbate schizophrenia-related behaviors in mice, *Neuroscience*, 2013, **33**, 7654–7666, DOI: 10.1523/JNEUROSCI.0091-13.2013.

6 G. Fond, E. Bulzacka, L. Boyer, P. M. Llorca, O. Godin, L. Brunel, M. G. Andrianarisoa, B. Aouizerate, F. Berna, D. Capdevielle, I. Chereau, H. Denizot, J. M. Dorey, C. Dubertret, J. Dubreucq, C. Faget, F. Gabayet, Y. Le Strat, J. A. Micoulaud-Franchi, D. Misdrahi, R. Rey, R. Richieri, M. Roger, C. Passerieux, A. Schandrin, M. Urbach, P. Vidalhet, F. Schurhoff, M. Leboyer and G. FondaMental, Academic Centers of Expertise for Schizophrenia, Birth by cesarean section and schizophrenia: results from the multicenter FACE-SZ data-set, *Eur. Arch. Psychiatry Clin. Neurosci.*, 2017, **267**, 587–594, DOI: 10.1007/s00406-016-0708-3.

7 A. Moya-Perez, P. Luczynski, I. B. Renes, S. Wang, Y. Borre, C. Anthony Ryan, J. Knol, C. Stanton, T. G. Dinan and J. F. Cryan, Intervention strategies for cesarean section-induced alterations in the microbiota-gut-brain axis, *Nutr. Rev.*, 2017, **75**, 225–240, DOI: 10.1093/nutrit/nuw069.

8 A. Cotillard, S. P. Kennedy, L. C. Kong, E. Prifti, N. Pons, E. Le Chatelier, M. Almeida, B. Quinquis, F. Levenez, N. Galleron, S. Gougis, S. Rizkalla, J. M. Batto, P. Renault, Consortium ANR MicroObes, J. Dore, J. D. Zucker, K. Clement and S. D. Ehrlich, Dietary intervention impact on gut microbial gene richness, *Nature*, 2013, **500**, 585–588, DOI: 10.1038/nature12480.

9 E. Y. Hsiao, S. W. McBride, S. Hsien, G. Sharon, E. R. Hyde, T. McCue, J. A. Codelli, J. Chow, S. E. Reisman, J. F. Petrosino, P. H. Patterson and S. K. Mazmanian, Microbiota modulate behavioral and physiological abnormalities associated with neurodevelopmental disorders, *Cell*, 2013, **155**, 1451–1463, DOI: 10.1016/j.cell.2013.11.024.

10 S. Cussotto, K. V. Sandhu, T. G. Dinan and J. F. Cryan, The Neuroendocrinology of the Microbiota-Gut-Brain Axis: A Behavioural Perspective, *Front. Neuroendocrinol.*, 2018, **51**, 80–101, DOI: 10.1016/j.yfrne.2018.04.002.

11 C. N. Heiss and L. E. Olofsson, The role of the gut microbiota in development, function and disorders of the central nervous system and the enteric nervous system, *J. Neuroendocrinol.*, 2019, **31**, e12684, DOI: 10.1111/jne.12684.

12 X. Yuan, Y. Kang, C. Zhuo, X. F. Huang and X. Song, The gut microbiota promotes the pathogenesis of schizophrenia via multiple pathways, *Biochem. Biophys. Res. Commun.*, 2019, **512**, 373–380, DOI: 10.1016/j.bbrc.2019.02.152.

13 P. Zheng, B. Zeng, M. Liu, J. Chen, J. Pan, Y. Han, Y. Liu, K. Cheng, C. Zhou, H. Wang, X. Zhou, S. Gui, S. W. Perry, M. L. Wong, J. Licinio, H. Wei and P. Xie, The gut microbiome from patients with schizophrenia modulates the glutamate-glutamine-GABA cycle and schizophrenia-relevant behaviors in mice, *Sci. Adv.*, 2019, **5**, eaau8317, DOI: 10.1126/sciadv.aau8317.

14 F. Zhu, R. Guo, W. Wang, Y. Ju, Q. Wang, Q. Ma, Q. Sun, Y. Fan, Y. Xie, Z. Yang, Z. Jie, B. Zhao, L. Xiao, L. Yang, T. Zhang, B. Liu, L. Guo, X. He, Y. Chen, C. Chen, C. Gao, X. Xu, H. Yang, J. Wang, Y. Dang, L. Madsen, S. Brix, K. Kristiansen, H. Jia and X. Ma, Transplantation of microbiota from drug-free patients with schizophrenia causes schizophrenia-like abnormal behaviors and dysregulated kynurenine metabolism in mice, *Mol. Psychiatry*, 2020, **25**, 2905–2918, DOI: 10.1038/s41380-019-0475-4.

15 S. A. Buffington, G. V. Di Prisco, T. A. Auchtung, N. J. Ajami, J. F. Petrosino and M. Costa-Mattioli, Microbial Reconstitution Reverses Maternal Diet-Induced Social and Synaptic Deficits in Offspring, *Cell*, 2016, **165**, 1762–1775, DOI: 10.1016/j.cell.2016.06.001.

16 N. Yuan, Y. Chen, Y. Xia, J. Dai and C. Liu, Inflammation-related biomarkers in major psychiatric disorders: a cross-disorder assessment of reproducibility and specificity in 43 meta-analyses, *Transl. Psychiatry*, 2019, **9**, 233, DOI: 10.1038/s41398-019-0570-y.

17 M. C. Opazo, E. M. Ortega-Rocha, I. Coronado-Arrazola, L. C. Bonifaz, H. Boudin, M. Neunlist, S. M. Bueno, A. M. Kalergis and C. A. Riedel, Intestinal Microbiota Influences Non-intestinal Related Autoimmune Diseases, *Front. Microbiol.*, 2018, **9**, 432, DOI: 10.3389/fmicb.2018.00432.

18 M. C. Marrone and R. Coccurello, Dietary Fatty Acids and Microbiota-Brain Communication in Neuropsychiatric Diseases, *Biomolecules*, 2019, **10**, 12, DOI: 10.3390/biom10010012.

19 D. Ni, W. Xu, Y. Zhu, W. Zhang, T. Zhang, C. Guang and W. Mu, Inulin and its enzymatic production by inulosucrase: Characteristics, structural features, molecular modifications and applications, *Biotechnol. Adv.*, 2019, **37**, 306–318, DOI: 10.1016/j.biotechadv.2019.01.002.

20 K. Li, L. Zhang, J. Xue, X. Yang, X. Dong, L. Sha, H. Lei, X. Zhang, L. Zhu, Z. Wang, X. Li, H. Wang, P. Liu, Y. Dong and L. He, Dietary inulin alleviates diverse stages of type 2 diabetes mellitus via anti-inflammation and modulating gut microbiota in db/db mice, *Food Funct.*, 2019, **10**, 1915–1927, DOI: 10.1039/c8fo02265h.

21 Q. Zhang, H. Yu, X. Xiao, L. Hu, F. Xin and X. Yu, Inulin-type fructan improves diabetic phenotype and gut microbiota profiles in rats, *PeerJ*, 2018, **6**, e4446, DOI: 10.7717/peerj.4446.

22 X. Song, L. Zhong, N. Lyu, F. Liu, B. Li, Y. Hao, Y. Xue, J. Li, Y. Feng, Y. Ma, Y. Hu and B. Zhu, Inulin Can Alleviate

Metabolism Disorders in ob/ob Mice by Partially Restoring Leptin-related Pathways Mediated by Gut Microbiota, *Genomics, Proteomics Bioinf.*, 2019, **17**, 64–75, DOI: 10.1016/j.gpb.2019.03.001.

23 W. Akram, N. Garud and R. Joshi, Role of inulin as prebiotics on inflammatory bowel disease, *Drug Discoveries Ther.*, 2019, **13**, 1–8, DOI: 10.5582/ddt.2019.01000.

24 T. Pattananandecha, S. Sirilun, Y. Duangjitcharoen, B. S. Sivamaruthi, P. Suwannalert, S. Peerajan and C. Chaiyasut, Hydrolysed inulin alleviates the azoxymethane-induced preneoplastic aberrant crypt foci by altering selected intestinal microbiota in Sprague-Dawley rats, *Pharm. Biol.*, 2016, **54**, 1596–1605, DOI: 10.3109/13880209.2015.1110597.

25 X. Yang, F. He, Y. Zhang, J. Xue, K. Li, X. Zhang, L. Zhu, Z. Wang, H. Wang and S. Yang, Inulin Ameliorates Alcoholic Liver Disease via Suppressing LPS-TLR4-Mpsi Axis and Modulating Gut Microbiota in Mice, *Alcohol.: Clin. Exp. Res.*, 2019, **43**, 411–424, DOI: 10.1111/acer.13950.

26 Z. Wang, X. Zhang, L. Zhu, X. Yang, F. He, T. Wang, T. Bao, H. Lu, H. Wang and S. Yang, Inulin alleviates inflammation of alcoholic liver disease via SCFAs-inducing suppression of M1 and facilitation of M2 macrophages in mice, *Int. Immunopharmacol.*, 2020, **78**, 106062, DOI: 10.1016/j.intimp.2019.106062.

27 J. Yu, D. Qi, M. Xing, R. Li, K. Jiang, Y. Peng and D. Cui, MK-801 induces schizophrenic behaviors through downregulating Wnt signaling pathways in male mice, *Brain Res.*, 2011, **1385**, 281–292, DOI: 10.1016/j.brainres.2011.02.039.

28 G. Krishna and Muralidhara, Inulin supplementation during gestation mitigates acrylamide-induced maternal and fetal brain oxidative dysfunctions and neurotoxicity in rats, *Neurotoxicol. Teratol.*, 2015, **49**, 49–58, DOI: 10.1016/j.ntt.2015.03.003.

29 D. Wang, Y. Noda, Y. Zhou, A. Nitta, H. Furukawa and T. Nabeshima, Synergistic effect of galantamine with risperidone on impairment of social interaction in phencyclidine-treated mice as a schizophrenic animal model, *Neuropharmacology*, 2007, **52**, 1179–1187, DOI: 10.1016/j.neuropharm.2006.12.007.

30 L. Legroux, C. L. Pittet, D. Beauseigle, G. Deblois, A. Prat and N. Arbour, An optimized method to process mouse CNS to simultaneously analyze neural cells and leukocytes by flow cytometry, *J. Neurosci. Methods*, 2015, **247**, 23–31, DOI: 10.1016/j.jneumeth.2015.03.021.

31 B. Golofast and K. Vales, The connection between microbiome and schizophrenia, *Neurosci. Biobehav. Rev.*, 2020, **108**, 712–731, DOI: 10.1016/j.neubiorev.2019.12.011.

32 J. R. Kelly, C. Minuto, J. F. Cryan, G. Clarke and T. G. Dinan, The role of the gut microbiome in the development of schizophrenia, *Schizophr. Res.*, 2020, DOI: 10.1016/j.schres.2020.02.010.

33 J. Qin, R. Li, J. Raes, M. Arumugam, K. S. Burgdorf, C. Manichanh, T. Nielsen, N. Pons, F. Levenez, T. Yamada, D. R. Mende, J. Li, J. Xu, S. Li, D. Li, J. Cao, B. Wang, H. Liang, H. Zheng, Y. Xie, J. Tap, P. Lepage, M. Bertalan, J. M. Batto, T. Hansen, D. Le Paslier, A. Linneberg, H. B. Nielsen, E. Pelletier, P. Renault, T. Sicheritz-Ponten, K. Turner, H. Zhu, C. Yu, S. Li, M. Jian, Y. Zhou, Y. Li, X. Zhang, S. Li, N. Qin, H. Yang, J. Wang, S. Brunak, J. Doré, F. Guarner, K. Kristiansen, O. Pedersen, J. Parkhill, J. Weissenbach, M. Consortium, P. Bork, S. D. Ehrlich and J. Wang, A human gut microbial gene catalogue established by metagenomic sequencing, *Nature*, 2010, **464**, 59–65, DOI: 10.1038/nature08821.

34 B. Flemer, N. Gaci, G. Borrel, I. R. Sanderson, P. P. Chaudhary, W. Tottey, P. W. O'Toole and J. F. Brugère, Fecal microbiota variation across the lifespan of the healthy laboratory rat, *Gut Microbes*, 2017, **8**, 428–439, DOI: 10.1080/19490976.2017.1334033.

35 A. Slyepchenko, M. Maes, F. N. Jacka, C. A. Köhler, T. Barichello, R. S. McIntyre, M. Berk, I. Grande, J. A. Foster, E. Vieta and A. F. Carvalho, Gut Microbiota, Bacterial Translocation, and Interactions with Diet: Pathophysiological Links between Major Depressive Disorder and Non-Communicable Medical Comorbidities, *Psychother. Psychosom.*, 2017, **86**, 31–46, DOI: 10.1159/000448957.

36 E. S. Chambers, C. S. Byrne, D. J. Morrison, K. G. Murphy, T. Preston, C. Tedford, I. Garcia-Perez, S. Fountana, J. I. Serrano-Contreras, E. Holmes, C. J. Reynolds, J. F. Roberts, R. J. Boyton, D. M. Altmann, J. A. K. McDonald, J. R. Marchesi, A. N. Akbar, N. E. Riddell, G. A. Wallis and G. S. Frost, Dietary supplementation with inulin-propionate ester or inulin improves insulin sensitivity in adults with overweight and obesity with distinct effects on the gut microbiota, plasma metabolome and systemic inflammatory responses: a randomised cross-over trial, *Gut*, 2019, **68**, 1430–1438, DOI: 10.1136/gutjnl-2019-318424.

37 L. J. Myhill, S. Stolzenbach, T. V. A. Hansen, K. Skovgaard, C. R. Stensvold, L. O. Andersen, P. Nejsum, H. Mejer, S. M. Thamsborg and A. R. Williams, Trichuris suisMucosal Barrier and Th2 Immune Responses Are Enhanced by Dietary Inulin in Pigs Infected With, *Front. Immunol.*, 2018, **9**, 2557, DOI: 10.3389/fimmu.2018.02557.

38 E. A. Barka, P. Vatsa, L. Sanchez, N. Gaveau-Vaillant, C. Jacquard, J. P. Meier-Kolthoff, H. Klenk, C. Clément, Y. Ouhdouch and G. P. Wezel, Taxonomy, Physiology, and Natural Products of Actinobacteria, *Microbiol. Mol. Biol. Rev.*, 2015, **80**, 1–43, DOI: 10.1128/MMBR.00019-15.

39 F. Guarner, Studies with inulin-type fructans on intestinal infections, permeability, and inflammation, *J. Nutr.*, 2007, **137**, 2568S–2571S, DOI: 10.1093/jn/137.11.2568S.

40 S. Claus, Inulin prebiotic: is it all about bifidobacteria?, *Gut*, 2017, **66**, 1883–1884, DOI: 10.1136/gutjnl-2017-313800.

41 B. Schroeder, G. Birchenough, M. Ståhlman, L. Arike, M. Johansson, G. Hansson and F. Bäckhed, Bifidobacteria or Fiber Protects against Diet-Induced Microbiota-Mediated Colonic Mucus Deterioration, *Cell Host Microbe*, 2018, **23**, 27–40.e7, DOI: 10.1016/j.chom.2017.11.004.

42 D. Anzawa, T. Mawatari, Y. Tanaka, M. Yamamoto, T. Genda, S. Takahashi, T. Nishijima, H. Kamasaka, S. Suzuki and T. Kuriki, Effects of synbiotics containing Bifidobacterium animalis subsp. lactis GCL2505 and inulin on intestinal bifidobacteria: A randomized, placebo-controlled, crossover study, *Food Sci. Nutr.*, 2019, **7**, 1828–1837, DOI: 10.1002/fsn3.1033.

43 T. Zelante, R. G. Iannitti, C. Cunha, A. De Luca, G. Giovannini, G. Pieraccini, R. Zecchi, C. D'Angelo, C. Massi-Benedetti, F. Fallarino, A. Carvalho, P. Puccetti and L. Romani, Tryptophan catabolites from microbiota engage aryl hydrocarbon receptor and balance mucosal reactivity via interleukin-22, *Immunity*, 2013, **39**, 372–385, DOI: 10.1016/j.immuni.2013.08.003.

44 D. Feng, H. Zhang, X. Jiang, J. Zou, Q. Li, H. Mai, D. Su, W. Ling and X. Feng, Bisphenol A exposure induces gut microbiota dysbiosis and consequent activation of gut-liver axis leading to hepatic steatosis in CD-1 mice, *Environ. Pollut.*, 2020, **265**, 114880, DOI: 10.1016/j.envpol.2020.114880.

45 A. Everard, C. Belzer, L. Geurts, J. P. Ouwerkerk, C. Druart, L. B. Bindels, Y. Guiot, M. Derrien, G. G. Muccioli, N. M. Delzenne, W. M. de Vos and P. D. Cani, Cross-talk between Akkermansia muciniphila and intestinal epithelium controls diet-induced obesity, *Proc. Natl. Acad. Sci. U. S. A.*, 2013, **110**, 9066–9071, DOI: 10.1073/pnas.1219451110.

46 H. Nishiwaki, M. Ito, T. Ishida, T. Hamaguchi, T. Maeda, K. Kashihara, Y. Tsuboi, J. Ueyama, T. Shimamura, H. Mori, K. Kurokawa, M. Katsuno, M. Hirayama and K. Ohno, Meta-Analysis of Gut Dysbiosis in Parkinson's Disease, *Mov. Disord.*, 2020, **35**, 1626–1635, DOI: 10.1002/mds.28119.

47 M. S. Desai, A. M. Seekatz, N. M. Koropatkin, N. Kamada, C. A. Hickey, M. Wolter, N. A. Pudlo, S. Kitamoto, N. Terrapon, A. Muller, V. B. Young, B. Henrissat, P. Wilmes, T. S. Stappenbeck, G. Núñez and E. C. Martens, A Dietary Fiber-Deprived Gut Microbiota Degrades the Colonic Mucus Barrier and Enhances Pathogen Susceptibility, *Cell*, 2016, **167**, 1339–1353.e21, DOI: 10.1016/j.cell.2016.10.043.

48 A. Fasano, Intestinal permeability and its regulation by zonulin: diagnostic and therapeutic implications, *Clin. Gastroenterol. Hepatol.*, 2012, **10**, 1096–1100, DOI: 10.1016/j.cgh.2012.08.012.

49 A. Fasano and T. Shea-Donohue, Mechanisms of disease: the role of intestinal barrier function in the pathogenesis of gastrointestinal autoimmune diseases, *Nat. Rev. Gastroenterol. Hepatol.*, 2005, **2**, 416–422, DOI: 10.1038/ncpgasthep0259.

50 D. Delbue, D. Cardoso-Silva, F. Branchi, A. Itzlinger, M. Letizia, B. Siegmund and M. Schumann, Celiac Disease Monocytes Induce a Barrier Defect in Intestinal Epithelial Cells, *Int. J. Mol. Sci.*, 2019, **20**, 5597, DOI: 10.3390/ijms20225597.

51 M. Vivinus-Nébot, G. Frin-Mathy, H. Bzioueche, R. Dainese, G. Bernard, R. Anty, J. Filippi, M. C. Saint-Paul, M. K. Tulic, V. Verhasselt, X. Hébuterne and T. Piche, Functional bowel symptoms in quiescent inflammatory bowel diseases: role of epithelial barrier disruption and low-grade inflammation, *Gut*, 2014, **63**, 744–752, DOI: 10.1136/gutjnl-2012-304066.

52 S. de Kort, D. Keszthelyi and A. A. Masclee, Leaky gut and diabetes mellitus: what is the link?, *Obes. Rev.*, 2011, **12**, 449–458, DOI: 10.1111/j.1467-789X.2010.00845.x.

53 V. Braniste, M. Al-Asmakh, C. Kowal, F. Anuar, A. Abbaspour, M. Tóth, A. Korecka, N. Bakocevic, L. G. Ng, N. L. Guan, P. Kundu, B. Gulyás, C. Halldin, K. Hultenby, H. Nilsson, H. Hebert, B. T. Volpe, B. Diamond and S. Pettersson, The gut microbiota influences blood-brain barrier permeability in mice, *Sci. Transl. Med.*, 2014, **6**, 263ra158, DOI: 10.1126/scitranslmed.3009759.

54 J. Xue, X. Li, P. Liu, K. Li, L. Sha, X. Yang, L. Zhu, Z. Wang, Y. Dong, L. Zhang, H. Lei, X. Zhang, X. Dong and H. Wang, Inulin and metformin ameliorate polycystic ovary syndrome via anti-inflammation and modulating gut microbiota in mice, *Endocr. J.*, 2019, **66**, 859–870, DOI: 10.1507/endocrj.EJ18-0567.

55 V. Rothhammer, I. D. Mascanfroni, L. Bunse, M. C. Takenaka, J. E. Kenison, L. Mayo, C. C. Chao, B. Patel, R. Yan, M. Blain, J. I. Alvarez, H. Kébir, N. Anandasabapathy, G. Izquierdo, S. Jung, N. Obholzer, N. Pochet, C. B. Clish, M. Prinz, A. Prat, J. Antel and F. J. Quintana, Type I interferons and microbial metabolites of tryptophan modulate astrocyte activity and central nervous system inflammation via the aryl hydrocarbon receptor, *Nat. Med.*, 2016, **22**, 586–597, DOI: 10.1038/nm.4106.

56 B. Leonard and M. Maes, Mechanistic explanations how cell-mediated immune activation, inflammation and oxidative and nitrosative stress pathways and their sequels and concomitants play a role in the pathophysiology of unipolar depression, *Neurosci. Biobehav. Rev.*, 2012, **36**, 764–785, DOI: 10.1016/j.neubiorev.2011.12.005.

57 M. Cowan and P. WA, Microglia: Immune Regulators of Neurodevelopment, *Front. Immunol.*, 2018, **9**, 2576, DOI: 10.3389/fimmu.2018.02576.

58 D. AM, Neurotrophins: neurotrophic modulation of neurite growth, *Curr. Biol.*, 2000, **10**, R198–R200, DOI: 10.1016/s0960-9822(00)00351-1.

59 D. Niculescu, K. Michaelsen-Preusse, Ü. Güner, R. van Dorland, C. J. Wierenga and C. Lohmann, A BDNF-Mediated Push-Pull Plasticity Mechanism for Synaptic Clustering, *Cell Rep.*, 2018, **24**, 2063–2074, DOI: 10.1016/j.celrep.2018.07.073.

60 H. Feng, C. Wang, W. He, X. Wu, S. Li, Z. Zeng, M. Wei and B. He, Roflumilast ameliorates cognitive impairment in APP/PS1 mice via cAMP/CREB/BDNF signaling and anti-neuroinflammatory effects, *Metab. Brain Dis.*, 2019, **34**, 583–591, DOI: 10.1007/s11011-018-0374-4.

61 S. Williams, L. Chen, H. M. Savignac, G. Tzortzis, D. C. Anthony and P. W. Burnet, Neonatal prebiotic (BGOS) supplementation increases the levels of synaptophysin,

GluN2A-subunits and BDNF proteins in the adult rat hippocampus, *Synapse*, 2016, **70**, 121–124, DOI: 10.1002/syn.21880.

62 F. Islam, B. H. Mulsant, A. N. Voineskos and T. K. Rajji, Brain-Derived Neurotrophic Factor Expression in Individuals With Schizophrenia and Healthy Aging: Testing the Accelerated Aging Hypothesis of Schizophrenia, *Curr. Psychiatry Rep.*, 2017, **19**, 36, DOI: 10.1007/s11920-017-0794-6.

63 B. Lamas, M. L. Richard, V. Leducq, H. P. Pham, M. L. Michel, G. Da Costa, C. Bridonneau, S. Jegou, T. W. Hoffmann, J. M. Natividad, L. Brot, S. Taleb, A. Couturier-Maillard, I. Nion-Larmurier, F. Merabtene, P. Seksik, A. Bourrier, J. Cosnes, B. Ryffel, L. Beaugerie, J. M. Launay, P. Langella, R. J. Xavier and H. Sokol, CARD9 impacts colitis by altering gut microbiota metabolism of tryptophan into aryl hydrocarbon receptor ligands, *Nat. Med.*, 2016, **22**, 598–605, DOI: 10.1038/nm.4102.

64 A. Agus, J. Planchais and H. Sokol, Gut Microbiota Regulation of Tryptophan Metabolism in Health and Disease, *Cell Host Microbe*, 2018, **23**, 716–724, DOI: 10.1016/j.chom.2018.05.003.

65 G. Morris, M. Berk, A. Carvalho, J. R. Caso, Y. Sanz, K. Walder and M. Maes, The Role of the Microbial Metabolites Including Tryptophan Catabolites and Short Chain Fatty Acids in the Pathophysiology of Immune-Inflammatory and Neuroimmune Disease, *Mol. Neurobiol.*, 2017, **54**, 4432–4451, DOI: 10.1007/s12035-016-0004-2.

66 J. M. Yano, K. Yu, G. P. Donaldson, G. G. Shastri, P. Ann, L. Ma, C. R. Nagler, R. F. Ismagilov, S. K. Mazmanian and E. Y. Hsiao, Indigenous bacteria from the gut microbiota regulate host serotonin biosynthesis, *Cell*, 2015, **161**, 264–276, DOI: 10.1016/j.cell.2015.02.047.

67 H. M. Savignac, Y. Couch, M. Stratford, D. M. Bannerman, G. Tzortzis, D. C. Anthony and P. W. J. Burnet, Prebiotic administration normalizes lipopolysaccharide (LPS)-induced anxiety and cortical 5-HT2A receptor and IL1-β levels in male mice, *Brain Behav. Immun.*, 2016, **52**, 120–131, DOI: 10.1016/j.bbi.2015.10.007.

68 C. C. Watkins and S. R. Andrews, Clinical studies of neuroinflammatory mechanisms in schizophrenia, *Schizophr. Res.*, 2016, **176**, 14–22, DOI: 10.1016/j.schres.2015.07.018.

69 N. Müller, Immunology of schizophrenia, *NeuroImmunoModulation*, 2014, **21**, 109–116, DOI: 10.1159/000356538.

70 F. Zhu, Y. Ju, W. Wang, Q. Wang, R. Guo, Q. Ma, Q. Sun, Y. Fan, Y. Xie, Z. Yang, Z. Jie, B. Zhao, L. Xiao, L. Yang, T. Zhang, J. Feng, L. Guo, X. He, Y. Chen, C. Chen, C. Gao, X. Xu, H. Yang, J. Wang, Y. Dang, L. Madsen, S. Brix, K. Kristiansen, H. Jia and X. Ma, Metagenome-wide association of gut microbiome features for schizophrenia, *Nat. Commun.*, 2020, **11**, 1612, DOI: 10.1038/s41467-020-15457-9.

71 Y. J. Chen, H. Wu, S. D. Wu, N. Lu, Y. T. Wang, H. N. Liu, L. Dong, T. T. Liu and X. Z. Shen, Parasutterella, in association with irritable bowel syndrome and intestinal chronic inflammation, *J. Gastroenterol. Hepatol.*, 2018, **33**, 1844–1852, DOI: 10.1111/jgh.14281.

72 C. A. Jones, D. J. Watson and K. C. Fone, Animal models of schizophrenia, *Br. J. Pharmacol.*, 2011, **164**, 1162–1194, DOI: 10.1111/j.1476-5381.2011.01386.x.

73 O. T. CM and W. JL, Closing the translational gap between mutant mouse models and the clinical reality of psychotic illness, *Neurosci. Biobehav. Rev.*, 2015, **58**, 19–35, DOI: 10.1016/j.neubiorev.2015.01.016.

74 H. M. Savignac, Y. Couch, M. Stratford, D. M. Bannerman, G. Tzortzis, D. C. Anthony and P. W. J. Burnet, Prebiotic administration normalizes lipopolysaccharide (LPS)-induced anxiety and cortical 5-HT2A receptor and IL1-beta levels in male mice, *Brain, Behav., Immun.*, 2016, **52**, 120–131, DOI: 10.1016/j.bbi.2015.10.007.

75 A. C. Kao, S. Spitzer, D. C. Anthony, B. Lennox and P. W. J. Burnet, Prebiotic attenuation of olanzapine-induced weight gain in rats: analysis of central and peripheral biomarkers and gut microbiota, *Transl. Psychiatry*, 2018, **8**, 66, DOI: 10.1038/s41398-018-0116-8.

76 J. L. Reilly, M. S. Harris, M. S. Keshavan and J. A. Sweeney, Adverse effects of risperidone on spatial working memory in first-episode schizophrenia, *Arch. Gen. Psychiatry*, 2006, **63**, 1189–1197, DOI: 10.1001/archpsyc.63.11.1189.

77 J. L. Reilly, M. S. Harris, T. T. Khine, M. S. Keshavan and J. A. Sweeney, Antipsychotic drugs exacerbate impairment on a working memory task in first-episode schizophrenia, *Biol. Psychiatry*, 2007, **62**, 818–821, DOI: 10.1016/j.biopsych.2006.10.031.

78 J. Mastropaolo, R. B. Rosse and S. I. Deutsch, Anabasine, a selective nicotinic acetylcholine receptor agonist, antagonizes MK-801-elicited mouse popping behavior, an animal model of schizophrenia, *Behav. Brain Res.*, 2004, **153**, 419–422, DOI: 10.1016/j.bbr.2003.12.023.

79 Y. Xiu, X. R. Kong, L. Zhang, X. Qiu, F. L. Chao, C. Peng, Y. Gao, C. X. Huang, S. R. Wang and Y. Tang, White matter injuries induced by MK-801 in a mouse model of schizophrenia based on NMDA antagonism, *Anat. Rec.*, 2014, **297**, 1498–1507, DOI: 10.1002/ar.22942.

80 S. Hiel, A. M. Neyrinck, J. Rodriguez, B. D. Pachikian, C. Bouzin, J. P. Thissen, P. D. Cani, L. B. Bindels and N. M. Delzenne, Inulin Improves Postprandial Hypertriglyceridemia by Modulating Gene Expression in the Small Intestine, *Nutrients*, 2018, **10**, 532, DOI: 10.3390/nu10050532.